

Synthesis of the DNA–[Ru(tpy)(dppz)(CH₃CN)]²⁺ Conjugates and Their Photo Cross-Linking Studies with the Complementary DNA Strand

Dimitri Ossipov,[†] Suresh Gohil,[‡] and Jyoti Chattopadhyaya^{*,†}

Contribution from the Department of Bioorganic Chemistry, Box 581, Biomedical Center, University of Uppsala, S-751 23 Uppsala, Sweden, and Department of Chemistry, Swedish University of Agricultural Sciences, Box 7015, Uppsala, Sweden

Received May 17, 2002

Abstract: We here report our studies on the conjugation of photoreactive Ru²⁺ complex to oligonucleotides (ODNs), which give a stable duplex with the complementary target DNA strand. These functionalized DNA duplexes bearing photoreactive Ru²⁺ complex can be specifically photolyzed to give the reactive aqua derivative, [Ru(tpy)(dppz)(H₂O)]²⁺–ODN (tpy = 2,2':6',2''-terpyridine; dppz = dipyrido[3,2-a:2',3'-c]-phenazine), in situ, which successfully cross-links to give photoproduct(s) in the duplex form with the target complementary DNA strand. Thus, the stable precursor of the aquaruthenium complex, the monofunctional polypyridyl ruthenium complex [Ru(tpy)(dppz)(CH₃CN)]²⁺, has been site-specifically tethered to ODN, for the first time, by both solid-phase synthesis and postsynthetic modifications. (i) In the first approach, pure 3'-[Ru(tpy)(dppz)(CH₃CN)]²⁺–ODN conjugate has been obtained in 42% overall yield (from the monomer blocks) by the automated solid-phase synthesis on a support labeled with [Ru(tpy)(dppz)Cl]⁺ complex with subsequent liberation of the crude conjugate from the support under mild conditions and displacement of the Cl[−] ligand by acetonitrile in the coordination sphere of the Ru²⁺ label. (ii) In the second approach, the single-modified (3'- or 5'- or middle-modified) or 3',5'-bis-modified Ru²⁺–ODN conjugates were prepared in 28–50% yield by an amide bond formation between an active ester of the metal complex and the ODNs conjugated with an amino linker. The pure conjugates were characterized unambiguously by ultraviolet–visible (UV–vis) absorption spectroscopy, enzymatic digestion followed by HPLC quantitation, polyacrylamide gel electrophoresis (PAGE), and mass spectrometry (MALDI-TOF as well as by ESI). [Ru(tpy)(dppz)(CH₃CN)]²⁺–ODNs form highly stabilized ODN·DNA duplexes compared to the unlabeled counterpart (ΔT_m varies from 8.4 to 23.6 °C) as a result of intercalation of the dppz moiety; they undergo clean and selective photodissociation of the CH₃CN ligand to give the corresponding aqua complex, [Ru(tpy)(dppz)(H₂O)]²⁺–ODNs (in the aqueous medium), which is evidenced from the change of their UV–vis absorption properties and the detection of the naked Ru²⁺–ODN ions generated in the course of the matrix-assisted laser desorption ionization time-of-flight (MALDI-TOF) mass spectrometric analysis. Thus, when [Ru(tpy)(dppz)(CH₃CN)]²⁺–ODN conjugate was hybridized to the complementary guanine (G)-rich target strand (**T**), and photolyzed in a buffer (pH 6.8), the corresponding aqua complex formed in situ immediately reacted with the G residue of the opposite strand, giving the cross-linked product. The highest yield (34%) of the photo cross-linked product obtained was with the ODN carrying two reactive Ru²⁺ centers at both 3'- and 5'-ends. For ODNs carrying only one Ru²⁺ complex, the yield of the cross-linked adduct in the corresponding duplex is found to decrease in the following order: 3'-Ru²⁺–ODN (22%) > 5'-Ru²⁺–ODN (9%) > middle-Ru²⁺–ODN (7%). It was also found that the photo cross-coupling efficiency of the tethered Ru²⁺ complex with the target **T** strand decreased as the stabilization of the resulting duplex increased: 3'-Ru²⁺–ODN (**VI·T**) ($\Delta T_m^b = 7$ °C) < 5'-Ru²⁺–ODN (**V·T**) ($\Delta T_m^b = 16$ °C) < middle-Ru²⁺–ODN (**VII·T**) ($\Delta T_m^b = 24.3$ °C, Table 2). This shows that, with the rigidly packed structure, as in the duplex with middle-Ru²⁺–ODN, the metal center flexibility is considerably reduced, and consequently the accessibility of target G residue by the aquaruthenium moiety becomes severely restricted, which results in a poor yield in the cross-coupling reaction. The cross-linked product was characterized by PAGE, followed by MALDI-TOF MS.

Introduction

Metal complexes can bind to DNA both via covalent¹ and noncovalent interactions.² In the first case, the substitution of a

labile ligand of the metal complex by a nucleophile in DNA leads to the metal–DNA adduct formation. Electron-rich DNA bases or phosphate groups are available for such direct covalent coordination to the metal center. In the case of substitution-inert stable metal complexes, only noncovalent binding modes, such as electrostatic binding, surface binding to grooved regions

* To whom correspondence should be addressed. E-mail: jyoti@boc.uu.se.

[†] University of Uppsala.

[‡] Swedish University of Agricultural Sciences.

of the DNA, or intercalation of planar aromatic ligand into the stacked base pairs, can be realized.³ In this category of inert complexes, polypyridyl complexes of Ru²⁺ and Rh³⁺ have been found to be valuable as luminescent reporters⁴ and DNA/RNA cleaving⁵ or cross-linking⁶ agents and also for the study of the long-range energy- and electron-transfer processes through the DNA,⁷ mainly due to their unique ground- and excited-state properties.⁸ On the other hand, because of their relative inertness toward ligand-substitution reactions, such complexes were also successfully conjugated to oligodeoxynucleotides (ODNs)⁹ to give the sequence specificity to complementary ODNs as well as to employ the light-activated properties of metal complex appending groups. These properties are of considerable interest for employing new tethered chemical or photo reagents to target DNA or RNA in a sequence-specific manner to give complementary addressed modification effect in a form of photocleavage of the target nucleic acid, which are elegantly shown by long-range oxidation of guanine in duplex DNA by tethered [Ru(phen)(bpy')(Me₂dppz)]²⁺ (artificial nucleases; bpy' = 4-carboxy-4'-methyl-2,2'-bipyridine and dppz = dipyrro[3,2-*a*:2',3'-*c*]phenazine)^{9f} or by photo cross-linking of two nucleic acid strands⁹ⁱ using tethered photoreactive [Ru(tap)₂(dip)]²⁺. Both effects, directed to viral sequences within double-stranded DNA or single-stranded mRNA, allow regulation of gene expression at the stage of transcription (antigene strategy)¹⁰ or translation (antisense strategy).¹¹

Clearly, highly reactive metal complexes containing reactive ligands should be able to give more desirable therapeutic effect because of irreversible covalent binding to DNA.¹² This has been proven for a wide range of functional metal complexes,

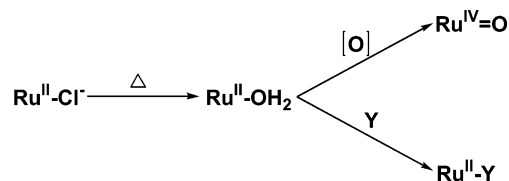


Figure 1.

such as cisplatin¹³ and its ruthenium analogues,¹⁴ *cis*- and *trans*-Ru^{II}Cl₂(DMSO)₄, Ru^{II}(bpy)₂Cl₂, Ru^{III}(tpy)Cl₃, and [Ru^{II}(NH₃)₅-Cl]Cl (DMSO = dimethyl sulfoxide; bpy = 2,2'-bipyridine; tpy = 2,2':6',2''-terpyridine), which showed antitumor activity and pronounced antimetastatic properties. There has also been much current interest in the chemistry of [Ru(tpy)(X)Cl]⁺ type of complexes (X = bpy, 1,10-phenanthroline (phen), and dppz)¹⁵ primarily due to the reactivity resulting from the relatively facile dissociation of the Ru²⁺-Cl⁻ bond (Figure 1).

The unique leading feature of aquaruthenium complexes, Ru²⁺-OH₂, is that they can bind to DNA presumably by replacement of the aqua ligand by nitrogen of a DNA heterocyclic base (this process is outlined by Ru^{II}-OH₂ → Ru^{II}-Y in Figure 1; Y = DNA base). Particularly, it has been shown that *intermolecular* reaction between [Ru(tpy)(X)(H₂O)]²⁺ and double-stranded DNA¹⁶ proceeds with a very poor yield ([Ru]_{bound}/[DNA-nucleotide] ≈ 0.02) because of high steric constraints caused by the incoming bulky Y group toward other polypyridyl ligands. Additionally, two-electron oxidation of aquaruthenium(II) generates powerful oxidizing oxoruthenium(IV) complexes (this process is outlined by Ru^{II}-OH₂ → Ru^{IV}=O in Figure 1), which have been used in a variety of oxidation reactions of organic substrates, including DNA cleavage through the C8-guanine/C1'-sugar oxidation.¹⁷

We here report our studies on the conjugation of photoreactive Ru²⁺ complex to ODN, which can form a stable duplex with the complementary target DNA, and subsequently can be photolyzed to produce the corresponding reactive aqua complex, Ru²⁺-OH₂, in situ, to cross-link with the complementary strand. Our initial results with the [Ru(phen)₂(dppz)]²⁺-tethered ODN showed that the tethering of the complex through the dppz group enhances the stability of the duplex by 12.8–23.4 °C as a result of threading of the dppz group through the duplex core;^{9m} hence, we chose the combination of tpy and dppz ligands to produce monofunctional [Ru(tpy)(dppz)(X)]²⁺ to tether with ODN. The following requirements should be fulfilled for design and synthesis of an ODN-[Ru(tpy)(dppz)(X)]²⁺ conjugate (X is a ligand, which upon activation gives the reactive aqua-Ru²⁺ complex): (1) It should be accessible by one of the usually

- (1) Billadeau, M. A.; Morrison, H. *Metal Ions in Biological Systems. In Photolytic Covalent Binding of Metal Complexes to DNA*; Sigel, A., Sigel, H., Ed.; Marcel Dekker Inc.: New York, 1996; Vol. 33, p 269.
- (2) Norden, B.; Lincoln, P.; Åkerman, B.; Tuite, E. *Metal Ions in Biological Systems. In DNA Interactions with Substitution-Inert Transition Metal Ion Complexes*; Sigel, A., Sigel, H., Ed.; Marcel Dekker Inc.: New York, 1996; Vol. 33, p 177.
- (3) Kelly, J. M.; Tossi, A. B.; McConnel, D. J.; OhUigin, C. *Nucleic Acids Res.* **1985**, *13*, 6017–6034.
- (4) Lackowicz, R. *Principles of Fluorescence Spectroscopy*; Kluwer Academic/Plenum Publishers: New York, 1999; pp 573–594.
- (5) Fleisher, M. B.; Waterman, K. C.; Turro, N. J.; Barton, J. K. *Inorg. Chem.* **1986**, *25*, 3549–3551.
- (6) Jacquet, L.; Kelly, J. M.; Kirsch-De Mesmaeker, A. *J. Chem. Soc., Chem. Commun.* **1995**, 913.
- (7) Holmlin, R. E.; Dandliker, P. J.; Barton, J. K. *Angew. Chem., Int. Ed. Engl.* **1997**, *36*, 2714–2730.
- (8) Ghosh, B. K.; Chakravorty, A. *Coord. Chem. Rev.* **1989**, *95*, 239.
- (9) (a) Kelly, J. M.; A Tossi, B.; McConnel, D. J.; OhUigin, C.; Hélène, C.; Le Doan, T. *In Free Radicals, Metal Ions and Biopolymers*; Beaumont, P. C., Deedle, D. J., Parsons, B. J., Rice-Evans, C., Eds.; Richelieu Press: London, 1989; pp 143–156. (b) Telsler, J.; Cruickshank, K. A.; Schanze, K. S.; Netzel, T. N. *J. Am. Chem. Soc.* **1989**, *111*, 7221–7226. (c) Bannwarth, W.; Schmidt, D. *Tetrahedron Lett.* **1989**, *30*, 1513–1516. (d) Jenkins, Y.; Barton, J. K. *J. Am. Chem. Soc.* **1992**, *114*, 8736–8738. (e) Meggers, E.; Kursch, D.; Giese, B. *Helv. Chim. Acta* **1997**, *80*, 640–652. (f) Arkin, M. R.; Stemp, E. D.; Pulver, S. C.; Barton, J. K. *Chem. Biol.* **1997**, *4*, 389–400. (g) Hurley, D. J.; Tor, Y. *J. Am. Chem. Soc.* **1998**, *120*, 2194–2195. (h) Wiederholt, K.; McLaughlin, L. W. *Nucleic Acids Res.* **1999**, *27*, 2487–2493. (i) Ortmans, L.; Content, S.; Boutonnet, N.; Kirsch-De Mesmaeker, A.; Bannwarth, W.; Constant, J.-F.; Defranco, E.; Lhomme, J. *Chem. Eur. J.* **1999**, *5*, 2712–2721. (j) Khan, S. I.; Beilstein, A. E.; Sykora, M.; Smith, G. D.; Hu, X.; Grinstaff, M. W. *Inorg. Chem.* **1999**, *38*, 3922–3925. (l) Rack, J. J.; Krider, E. S.; Meade, T. J. *J. Am. Chem. Soc.* **2000**, *122*, 6287–6288. (m) Ossipov, D.; Pradeepkumar, P. I.; Holmer, M.; Chattopadhyaya, J. *J. Am. Chem. Soc.* **2001**, *123*, 3551–3562. (n) Vargas-Baca, I.; Mitra, D.; Zulyniak, H. J.; Banerjee, J.; Sleiman, H. F. *Angew. Chem., Int. Ed.* **2001**, *40*, 4629–4632.
- (10) Thuong, N. T.; Hélène, C. *Angew. Chem., Int. Ed. Engl.* **1993**, *32*, 666–690.
- (11) de Mesmaeker, A.; Häner, R.; Martin, P.; Moser, H. E. *Acc. Chem. Res.* **1995**, *28*, 366–374.
- (12) Lippert, B.; Leng, M. *Metallopharmaceuticals I: DNA Interactions; In Role of Metal Ions in Antisense and Antigenic Strategies*; Clarke, M. J., Sadler, P. J., Eds.; Springer-Verlag: Berlin, Heidelberg, 1999; p 117.

- (13) Reedijk, J. *Chem. Commun.* **1996**, 801.
- (14) (a) Anagnostopoulou, A.; Moldrheim, E.; Katsaros, N.; Sletten, E. *J. Biol. Inorg. Chem.* **1999**, *4*, 199–208. (b) Esposito, G.; Cauci, S.; Fogolari, F.; Alessio, E.; Scocechi, M.; Quadrioglio, F.; Viglino, P. *Biochemistry* **1992**, *31*, 7094–7103. (c) Nováková, O.; Kašpárková, J.; Vrána, O.; van Vliet, P. M.; Reedijk, J.; Brabec, V. *Biochemistry* **1995**, *34*, 12369–12378. (d) van Vliet, P. M.; Toekimin, S. M. S.; Haasnoot, J. G.; Reedijk, J.; Nováková, O.; Vrána, O.; Brabec, V. *Inorg. Chim. Acta* **1995**, *231*, 57–64. (e) Bottomley, F. *Can. J. Chem.* **1977**, *55*, 2788.
- (15) Pramanik, N. C.; Pramanik, K.; Ghosh, P.; Bhattacharya, S. *Polyhedron* **1998**, *17*, 1525–1534.
- (16) (a) Grover, N.; Gupta, N.; Thorp, H. H. *J. Am. Chem. Soc.* **1992**, *114*, 3390–3393. (b) Grover, N.; Welch, T. W.; Fairlay, T. A.; Cory, M.; Thorp, H. H. *Inorg. Chem.* **1994**, *33*, 3544–3548. (c) Cheng, C.-C.; Lee, W.-L.; Su, J.-G.; Liu, C.-L. *J. Chin. Chem. Soc.* **2000**, *47*, 213–220.
- (17) (a) Carter, P. J.; Cheng, C.-C.; Thorp, H. H. *J. Am. Chem. Soc.* **1998**, *120*, 632–642. (b) Gupta, N.; Grover, N.; Neyhart, G. A.; Liang, W.; Singh, P.; Thorp, H. H. *Angew. Chem., Int. Ed. Engl.* **1992**, *31*, 1048–1050. (c) Thompson, M. S.; Meyer, T. J. *J. Am. Chem. Soc.* **1982**, *104*, 4106–4115.

exploited synthetic approaches (solid-phase synthesis or postsynthetic labeling) without any modification of the ligand X, (2) X should be chemically stable and substitution-inert toward nitrogenous bases (mostly guanine) of tethered ODN, and, finally, (3) it can be readily converted to the reactive ODN–Ru²⁺–OH₂ species without alteration of the ODN part at the final synthetic step. Recently, some efforts have been made to use such a methodology for covalent attachment of [Pt(NH₃)₂–(Y)Cl]⁺ species to ODN via solid-phase synthesis, where Y was 5'-amino linker¹⁸ or N7 (N3) of guanine (thymine) base¹⁹ of an ODN chain. In case of tethering through the 5'-amino linker, the dissociable Cl[–] ligand was generated by acidic substitution of cyclohexylmethylthymine group at the penultimate step of the ODN conjugate preparation, which limited the approach to only homopyrimidine 5'-ODN conjugates. In the case of tethering through the bases, chloroplatinated guanosine-3'-H-phosphonate (or thymidine-3'-H-phosphonate) monomer block was introduced in the course of ODN assembly, but the instability of Cl[–] ligand against N-donor compounds such as NH₃, used in the final ODN deprotection step, led to the formation of intrastrand cross-linked or other inactivated species not capable of reacting with the target molecules.

Our monofunctional [Ru(tpy)(dppz)(H₂O)]²⁺–ODN conjugates, which exhibit their reactivity toward guanine base of the complementary DNA strand, have been obtained in situ by photolytic activation of the thermally stable [Ru(tpy)(dppz)(CH₃CN)]²⁺–ODN precursors, in which *sn*-glycerol–tri(ethylene glycol) fused linker connects the dppz moiety of the metallocomplex to 3', or 5', or both termini of the 10mer ODN strand. The metallocomplex was also introduced at the internucleotide position of the ODN chain. The [Ru(tpy)(dppz)(CH₃CN)]²⁺ labeled ODNs have been prepared by postsynthetic modification of ODNs carrying amino linker at the desired position. This strategy has been proven to be valuable for incorporation of metalating species containing sensitive functionality. Derivatization at the 3'-end has also been performed by solid-phase synthesis starting from [Ru(tpy)(dppz)Cl]⁺–modified support. The reactivity of the photolytically prepared [Ru(tpy)(dppz)(H₂O)]²⁺–ODN conjugates toward the complementary strand in a duplex has been studied, and compared with the reactivity of the untethered [Ru(tpy)(dppz)(H₂O)](PF₆)₂ derivative.

Results and Discussion

(I) Chemistry of [Ru(tpy)(dppz)X]ⁿ⁺ (X = Cl[–], CH₃CN, H₂O). Ligand transformation and stability of subsequent complexes under the conditions of solid-phase synthesis, deprotection, and purification have been evaluated for a model compound [Ru(tpy)(dppz)Cl](PF₆) prior to the ODN-conjugate synthesis. The dissociation of Cl[–] ligand in aqueous medium to give Ru²⁺–OH₂ species is well-documented for numerous of the tetra-, tri-, di-, and monochlororuthenium(II) complexes.²⁰ The substitution of the aqua ligand by DNA constituents is believed to follow a reaction course similar to that found for

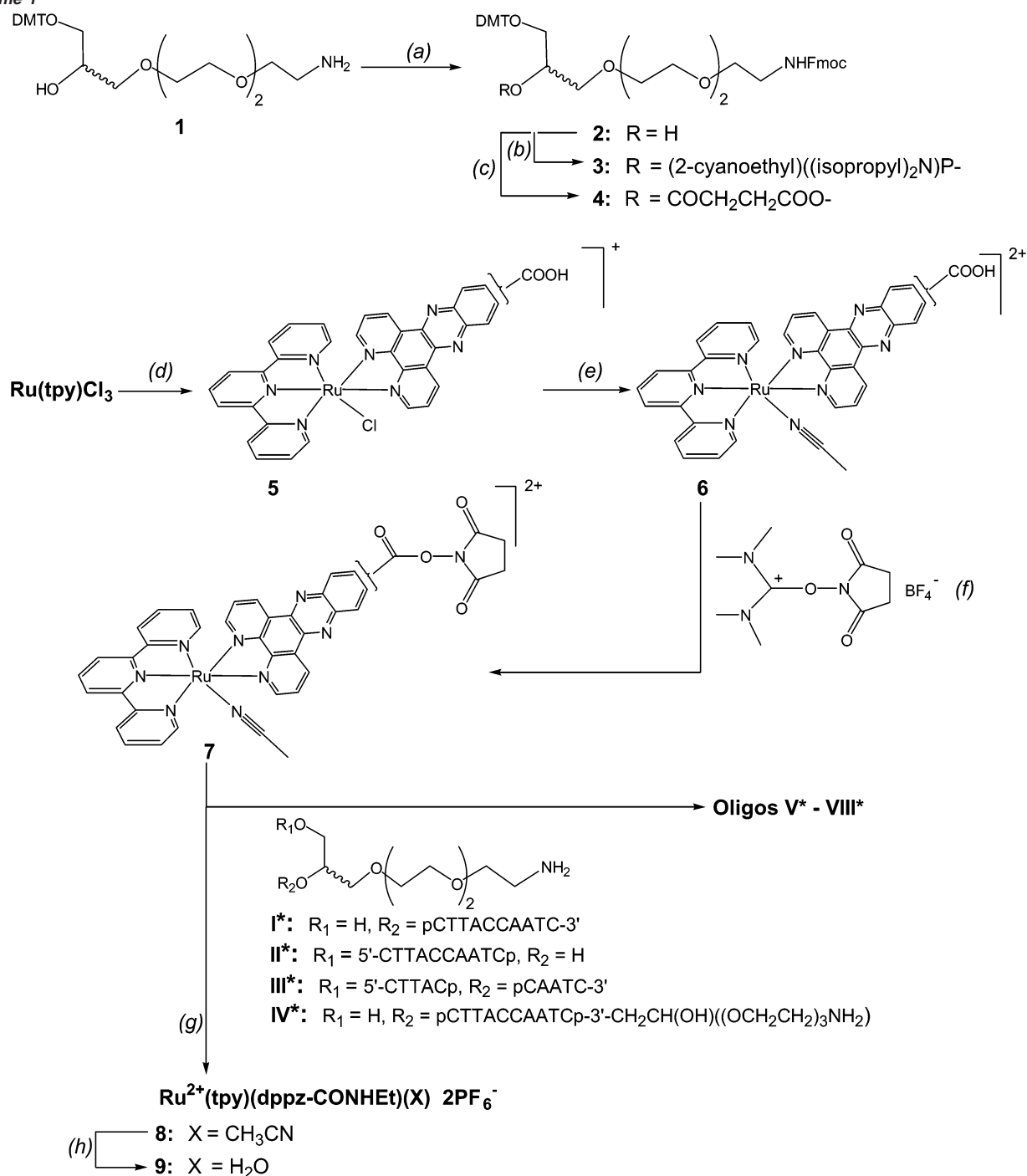
other transition metal complex based anticancer drug action.²¹ We found that [Ru(tpy)(dppz)Cl](PF₆) is kinetically stable in an acetone–H₂O mixture (1:1, v/v) at room temperature, but as the temperature increases (from 37 to 55 °C), the equilibrium is shifted, giving more aqua species. Subsequently, ¹H NMR spectroscopy analysis of [Ru(tpy)(dppz)Cl](PF₆) treated with aqueous NH₃ (25%) at 55 °C for 17 h indicated partial formation of two compounds assigned as products of Cl[–] substitution by H₂O and NH₃. Thus, our preliminary studies clearly showed that Cl[–] ligand cannot be considered as X of the precursor ODN–Ru²⁺–X conjugate, because it is not adequately stable in the aqueous media, which limits its manipulations in the course of ammonia deprotection and purification by standard procedures.

This has led us to find other ligands, which are thermally stable such as in [Ru(tpy)(bpy)X]²⁺, in which X is acetonitrile or pyridine.^{22a–c} The unique property of X in these [Ru(tpy)(bpy)X]²⁺ complexes is that they undergo photosubstitution reaction to give the corresponding aquaruthenium complex. Particularly, [Ru(tpy)(bpy)(CH₃CN)]²⁺ has been found^{22b} to be useful because it is thermally inert, and acetonitrile is a good, unidentate leaving group under light irradiation. For [Ru(tpy)(bpy)(CH₃CN)]²⁺ the photosubstitution of CH₃CN by solvent molecule has been examined in acetonitrile alone or in the presence of another nucleophile such as pyridine. These reactions have either shown ligand isomerization^{22c} or substitution of CH₃CN by pyridine.^{22b} One could assume similar photosubstitution of CH₃CN by H₂O in aqueous medium in the absence of any potential nucleophile. Indeed, we found that photolysis of [Ru(tpy)(dppz)(CH₃CN)](PF₆)₂ in an acetone–H₂O mixture (1:1, v/v) quantitatively yields [Ru(tpy)(dppz)(H₂O)](PF₆)₂ (see below). We have also examined the stability of [Ru(tpy)(dppz)(CH₃CN)](PF₆)₂ in acetone–concentrated aqueous ammonia mixture (1:1, v/v). Contrary to [Ru(tpy)(dppz)Cl](PF₆), the ancillary acetonitrile ligand in [Ru(tpy)(dppz)(CH₃CN)](PF₆)₂ was completely base hydrolyzed²³ to the corresponding amide ligand in 2 h at room temperature. This suggests that the Ru²⁺–NCCH₃ species cannot be used in the solid-phase ODN synthesis, because the basic removal condition is required both in the release of ODN from the solid support and in the deprotection of the amino or imide protecting groups. Hence, Ru²⁺–NCCH₃ species could be introduced only as a postsynthetic modification to already synthesized and deprotected ODN in solution.

(II) Synthesis of Ru²⁺–ODN Conjugates by Postsynthetic Labeling of Amino-Functionalized ODNs. On the basis of the above properties of [Ru(tpy)(dppz)X]ⁿ⁺ complexes (X = Cl[–], H₂O, CH₃CN), we have accomplished the synthesis of [Ru(tpy)(dppz)(CH₃CN)]²⁺–ODN conjugates by two alternative means, which have been subsequently used for photolytic activation to give finally reactive aquaruthenium(II)–ODN conjugates. In the first approach (Scheme 1), Ru²⁺–NCCH₃ complex was introduced to the ODN by the amide bond formation between *N*-hydroxysuccinimide ester (NHS ester) of

- (18) Schmidt, K. S.; Filippov, D. V.; Meeuwenoord, N. J.; van der Marel, G. A.; van Boom, J. H.; Lippert, B.; Reedijk, J. *Angew. Chem., Int. Ed.* **2000**, *39*, 375–377.
 (19) (a) Manchanda, R.; Dunham, S. U.; Lippard, S. J. *J. Am. Chem. Soc.* **1996**, *118*, 5144–5145. (b) Schliepe, J.; Berghoff, U.; Lippert, B.; Cech, D. *Angew. Chem., Int. Ed. Engl.* **1996**, *35*, 646–648.
 (20) Seddon, E. A.; Seddon, K. R. *The Chemistry of Ruthenium*; Elsevier: Amsterdam, 1984.

- (21) Gelasco, G.; Lippard, S. J. *Metallopharmaceuticals I: DNA Interactions. In Anticancer Activity of Cisplatin and Related Complexes*; Clarke, M. J., Sadler, P. J., Eds.; Springer-Verlag: Berlin, Heidelberg, 1999; p 117.
 (22) (a) Suen, H.-F.; Wilson, S. W.; Pomerantz, M.; Walsh, J. L. *Inorg. Chem.* **1989**, *28*, 786–791. (b) Hecker, C. R.; Fanwick, P. E.; McMillin, D. R. *Inorg. Chem.* **1991**, *30*, 659–666. (c) Laemmel, A.-C.; Collin, J.-P.; Sauvage, J.-P. *C. R. Acad. Sci. Paris* **2000**, *3*, 43–49.
 (23) Fagalde, F.; Lis de Katz, N. D.; Katz, N. E. *Polyhedron* **1997**, *16*, 1921–1923.

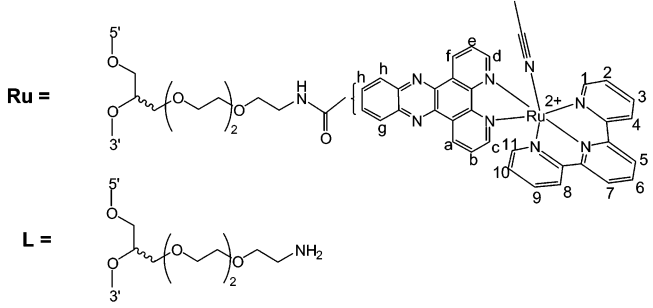
Scheme 1^a

^a (a) 9-Fluorenylmethyl chloroformate, (iPr)₂EtN, DMF, 1 h, 20 °C; (b) (2-CeO)((iPr)₂N)PCL, (iPr)₂EtN, CH₂Cl₂, 1 h, 20 °C; (c) succinic anhydride, DMAP, CH₂Cl₂, 5 h, 20 °C; (d) dipyrido[3,2-*a*:2',3'-*c*]phenazine-11-carboxylic acid, LiCl, Et₃N, 3:1 ethanol-water, 4 h, reflux; (e) 3:1 acetonitrile-water, 3.5 h, reflux; (f) *N,N,N',N'*-tetramethyl-*O*-(*N*-succinimidyl)uronium tetrafluoroborate, (iPr)₂EtN, DMF, 2 h, 20 °C; (g) 33% C₂H₅NH₂/ethanol, DMF, 2 h, 20 °C; (h) *hν*, 7:4 acetone-water, 2 h, 20 °C. (*) See Table 1 for abbreviations.

the complex [Ru(tpy)(dppz-COOH)(CH₃CN)]Cl₂ (**6**) and the amino-functionalized linker tethered to an oligonucleotide at the desired position. Compound **1**²⁴ has been used uniformly to incorporate the amino function with a long linker to either 3'- or 5'-terminal or between two nucleotides in the ODN. The amino group in **1** was first protected with *N*-fluorenylmethoxycarbonyl, affording **2** (67%). After conversion of **2** to the

phosphoramidite **3** (77%), it was used in the solid-phase synthesis, permitting the incorporation of amino linker **L** (Table 1) either between the two phosphodiester residues of the ODN or to the 5'-terminal of the ODN chain. Compound **2** was also treated with succinic anhydride to give the corresponding succinate block **4** (65%), which was then immobilized onto an aminopropyl-CPG support (49 μmol/g) and was used for the incorporation of the amino linker **L** at the 3'-terminal of the ODN. The amino-modified ODNs **I-IV** (Table 1), thus

(24) Ossipov, D.; Zamaratski, E.; Chattopadhyaya, J. *Helv. Chim. Acta* **1999**, *82*, 2186-2200.

Table 1. Synthetic Ru²⁺-Labeled ODN Conjugates and Their Target Oligo-DNA


oligo			yield (%)		compd abbrevn	
			solid-phase synthesis	postsynthetic labeling		
antisense ODNs	natural	5'-CTTACCAATC-3'	67		N	
	5'-modified	5'-L-pCTTACCAATC-3'	56		I	
	3'-modified	5'-Ru-pCTTACCAATC-3'			46	V
		5'-CTTACCAATCp-L-3'	59			II
	middle	5'-CTTACCAATCp-Ru-3'	69		51	VI
		5'-CTTACp-L-pCAATC-3'	87			III
		5'-CTTACp-Ru-pCAATC-3'			28	VII
5'-modified	5'-L-pCTTACCAATCp-L-3'	64			IV	
target 11mer	5'-Ru-pCTTACCAATCp-Ru-3'			34	VIII	
	5'-TGATTGGTAAG-3'		87		T	

prepared, were deprotected with concentrated ammonia (55 °C for 17 h) and purified by reverse-phase HPLC with a gradient of 5–50% CH₃CN containing 0.1 M triethylammonium acetate, pH 7.0.

The Ru²⁺-NCCH₃ complex **6** was synthesized in two steps,^{15,22b,c} Ru(tpy)Cl₃ → **5** (62%) → **6** (100%) (Scheme 1), and then it was coupled with the deprotected amino-modified ODNs in solution through the NHS ester **7** (93%) in the following manner: NHS ester **7** was prepared by treatment with *N,N,N',N'*-tetramethyl-*O*-(*N*-succinimidyl)uronium tetrafluoroborate in dry DMF. The reactivity of **7** as an activated ester was controlled by its reaction with ethylamine under anhydrous conditions (in dry dimethylformamide (DMF)), which afforded [Ru(tpy)(dppz-CONHEt)(CH₃CN)](PF₆)₂ (compound **8**) in 79% yield. Subsequently, the preparation of [Ru(tpy)(dppz)-(CH₃CN)]²⁺-ODN conjugates was undertaken. Thus, amino-modified ODNs **I–IV** at a concentration of 0.22 mmol/L with a 25-fold molar excess of **7** were vortexed in 33% CH₃CN/10 mmol/L sodium tetraborate (pH 8.5) at room temperature for 24 h in the dark. The reaction mixtures were then directly applied to the column packed with the cation exchange Sephadex SP C-25 resin and washed with 30% CH₃CN/H₂O to elute the crude ODN conjugates **V–VIII** (Table 1) from **7**. Eluted material was evaporated with the temperature not exceeding 30 °C and purified by reverse-phase HPLC under the same conditions as those employed for the purification of amine-modified ODNs.

Precautions should be taken in the pH adjustment of the reaction mixture, because at high pH the hydrolysis of the coordinated acetonitrile gives Ru²⁺-acetamide,²³ while at low pH competing hydrolysis of the NHS ester bond occurs.²⁵ Under our conditions, the yield of the coupling to give ODN conjugates **V–VIII** was 28–51%, which has not been optimized by using any other buffer system.

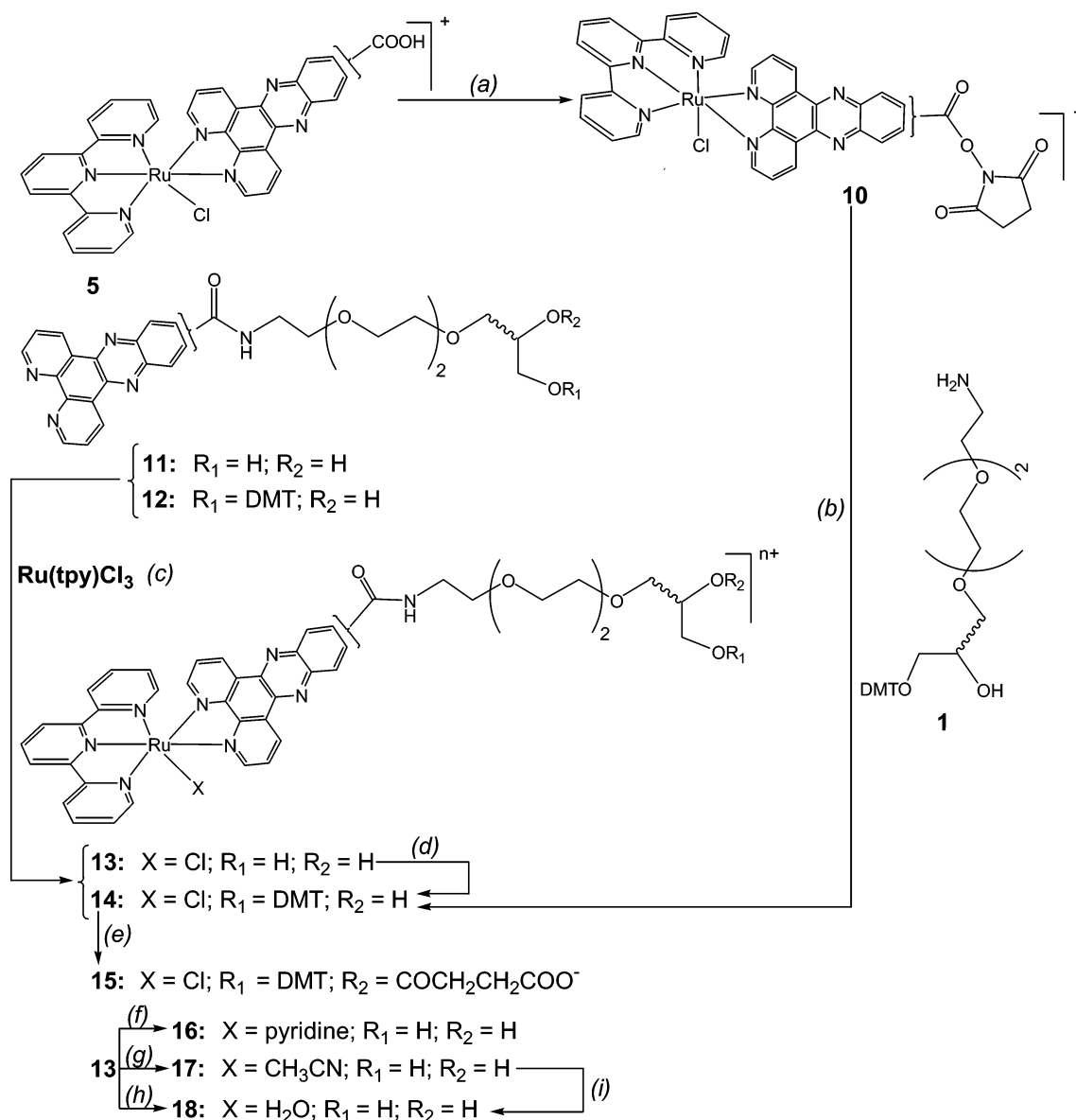
(III) Synthesis of Ru²⁺-ODN Conjugates by the Automated Synthesis Utilizing Ru²⁺-Labeled Solid Support.

In our attempt to synthesize [Ru(tpy)(dppz)(CH₃CN)]²⁺-ODN conjugates through the automated solid-phase synthesis, we have elaborated a different synthetic approach (Scheme 2). Recently, Meyer et al. have reported on the incorporation of the [Ru(tpy)(bpy)Cl]⁺ into polymers and peptides.²⁶ The Cl⁻ ligand was unaltered under conditions used for their chemical conversions. It was however clear to us (see above) that Cl⁻ ligand would not remain intact during the ODN assembly with 3'-[Ru(tpy)(dppz)Cl]⁺-modified solid support; hence, we planned our strategy such that it would allow us to substitute Cl⁻ by CH₃CN ligand. Compound **1** was linked (Scheme 2) to the Cl⁻ ligand containing complex, as in **5**, by either amide bond formation (**5** → **10** → **14** path) or by coordination reaction of Ru(tpy)Cl₃ with the functionalized dppz ligand **11** or **12** (**11** → **13** → **14** or **12** → **14** paths). In the first path, Cl⁻ containing [Ru(tpy)(dppz-COOH)Cl]⁺ complex **5** (analogue of **6**) was first activated and then coupled to the amine **1** in 52% overall yield using a procedure used for the coupling of complex **7** with ethylamine in dry DMF (Scheme 1). Alternatively, complex formation between Ru(tpy)Cl₃ and dppz-linker conjugate **11** afforded **13** (91%), in which the primary hydroxyl was protected with the 4,4'-dimethoxytrityl (DMT) group, giving finally compound **14** (56%). The reaction condition used for **11** → **13** allowed us to apply it also for the reaction with DMT-protected dppz-linker conjugate as in **12** → **14** (95%). Treatment of **14** with succinic anhydride produced the succinate **15** (62%). Following attachment of succinate **15** to the aminopropyl-CPG enabled us to prepare the [Ru(tpy)(dppz)Cl]⁺-modified solid support.

Appropriately tethered Ru²⁺-Cl⁻ complex **13** was found to undergo Cl⁻ ligand substitution by other ligands (X), such as pyridine, CH₃CN, or H₂O, under the reaction conditions usually

(25) Haugland, R. P. *Handbook of Fluorescent Probes and Research Chemicals*, 6th ed., Molecular Probes: Eugene, OR, 1996.

(26) (a) Hartshorn, S. M.; Maxwell, K. A.; White, P. S.; DeSimone, J. M.; Meyer, T. J. *Inorg. Chem.* **2001**, *40*, 601–606. (b) Serron, S. A.; Aldridge, W. S., III; Danell, R. M.; Meyer, T. J. *Tetrahedron Lett.* **2001**, *41*, 4039–4042.

Scheme 2^a

^a (a) *N,N,N',N'*-Tetramethyl-*O*-(*N*-succinimidyl)uronium tetrafluoroborate, (iPr)₂EtN, DMF, 2 h, 20 °C; (b) **1**, DMF, 2 h, 20 °C; (c) Ru(tpy)Cl₃, LiCl, Et₃N, 3:1 ethanol–water, 4 h, reflux; (d) 4,4'-dimethoxytrityl chloride, pyridine, 1.5 h, 20 °C; (e) succinic anhydride, DMAP CH₂Cl₂, 5 h, 20 °C; (f) 1:5:5 pyridine–ethanol–water, 5 h, reflux; (g) 3:1 acetonitrile–water, 3.5 h, reflux; (h) silver toluene-*p*-sulfonate, 3:1 acetone–water, 1 h, reflux; (i) hv, 7:4 acetone–water, 2 h, 20 °C.

employed^{22b,c,27} for the synthesis of [Ru(tpy)(NN)(X)]²⁺ complexes, where NN denotes a bidentate ligand. When **13** is heated in an aqueous solution, in the absence of any other coordinating species, the dissociation of Cl⁻ ligand takes place to afford aquaruthenium(II) complex **18** (75%), while the reaction in pyridine–H₂O or acetonitrile–H₂O mixtures affords **16** (70%) or **17** (70%), respectively (Scheme 2).

For the automated assembly of the 3'-[Ru(tpy)(dppz)Cl]⁺–ODN conjugate, the fast deprotecting 5'-*O*-(4,4'-dimethoxytrityl)-*N*⁴-isobutyryl-2'-deoxycytidine-3'-*O*-(β-cyanoethyl-*N,N*-diisopropyl)- and 5'-*O*-(4,4'-dimethoxytrityl)-*N*⁶-phenoxyacetyl-2'-deoxyadenosine-3'-*O*-(β-cyanoethyl-*N,N*-diisopropyl)phosphoramidites²⁸ were used, and the resulting ODNs were deprotected by ammonia treatment at room temperature (17 h) to

exclude thermal dissociation of the Ru²⁺–Cl⁻ bond and the subsequent ligand displacement. After filtration from the solid support the ammonia solution was concentrated in vacuo below 25 °C, and residual aqueous solution was finally lyophilized. The lyophilized material was dissolved in a CH₃CN–H₂O mixture (1:1, v/v) and heated at 55 °C for 17 h to substitute Cl⁻ with CH₃CN at the metal center to give the crude 3'-[Ru(tpy)(dppz)(NCCH₃)]²⁺–ODN conjugate **VI** (Table 1), which was then purified by reverse-phase HPLC under the conditions employed for the purification of amine-modified ODNs.

(IV) HPLC Purification, PAGE, UV–Vis Spectroscopy, and Enzymatic Digestion of Ru²⁺–ODN Conjugates. A

(28) (a) Sinha, N. D.; Biernat, J.; McManus, J.; Koster, H. *Nucleic Acids Res.* **1984**, *12*, 4539. (b) Sinha, N. D.; Biernat, J.; Koster, H. *Tetrahedron Lett.* **1983**, *24*, 5843.

(29) Onfelt, B.; Lincoln, P.; Norden, B. *J. Am. Chem. Soc.* **1999**, *121*, 10846–10847.

(27) Ho, C.; Che, C.-M.; Lau, T.-C. *J. Chem. Soc., Dalton. Trans.* **1990**, 967–970.

typical chromatogram of crude amino-linker modified ODN **II** ($R_t = 38.4$ min) is shown, as an example in Supporting Information (S), Figure S1(A). Coupling of **7** to the amino group of ODN **II** is indicated by consumption of the starting ODN ($R_t = 38.2$ min, Figure S1(B)) and appearance of two well-resolved product peaks ($R_t = 52.7$ and 54.4 min, Figure S1(B)). These peaks were assigned to diastereomeric $[\text{Ru}(\text{tpy})(\text{dppz})(\text{CH}_3\text{CN})]^{2+}$ -modified ODN **VI** (designated as **VIa** and **VIb** for the fractions eluted at 52.7 and 54.4 min, respectively), which was confirmed by comparison of their UV-vis spectral bands with the nontethered $[\text{Ru}(\text{tpy})(\text{dppz-L})(\text{CH}_3\text{CN})](\text{PF}_6)_2$ **17** (Figure S2). The A_{260}/A_{453} absorption ratio for these fractions (9.1) was also found to be higher than the corresponding ratio for the parent Ru^{2+} complex **17** (3.5), thereby reflecting the contribution of the DNA bases at 260 nm (see below for mass spectral evidence). Products **VIa** and **VIb** showed the metal-to-ligand charge transfer (MLCT) band at 453 nm, which is characteristic for the $[\text{Ru}(\text{tpy})(\text{bpy})(\text{CH}_3\text{CN})]^{2+}$ type of complexes.^{22b,c,23} The MLCT transition is very dependent on the nature of unidentate ligand X in the complexes of general formula $[\text{Ru}(\text{tpy})(\text{dppz-L})\text{X}]^{2+}$, as is clearly seen in Figure S3. It implies that the CH_3CN ligand has indeed remained intact in the course of the coupling reaction and purification under subdued light. Analysis of **VIa** and **VIb** by gel electrophoresis revealed (Figure 2B) that they migrate in a similar manner as retarded bands compared to the starting amino-modified ODN **II**, which, in turn, migrates slower than the native 10mer **N**. Clearly, the lower electrophoretic mobility of the metalated ODNs than the amino-linker-conjugated ODN **II** is due to the higher molecular weight (685 for $[\text{Ru}(\text{tpy})(\text{dppz-CO})(\text{N-CCH}_3)]^{2+}$ residue) and a decrease of the overall negative charge by 2 in the former.

Composition of **VIa** and **VIb** and the presence of the tethered Ru^{2+} complex was also confirmed by its degradation to nucleosides upon treatment with a mixture of snake venom phosphodiesterase (SVDP) and alkaline phosphatase (AP). Digestion of conjugates, followed by HPLC analysis, resulted in a chromatogram indicating the presence of three nucleosides expected for the sequence and strongly retarded species corresponding to the Ru^{2+} complex. The identity of peaks eluted at 9.5, 13.9, and 16.6 min to dC, T, and dA, respectively, was proven by comparison with retention times for an authentic mixture of nucleosides. Areas under these peaks were divided onto corresponding molar extinction coefficients for dC, T, and dA, and the ratio of normalized areas was found to be 4.1:3:2.9, which is close to the nucleoside composition in ODN **VI** (4:3:3).

The ODNs **V**, **VII**, and **VIII**, prepared postsynthetically from amino-modified ODNs **I**, **III**, and **IV**, respectively, were purified and characterized in a manner similar to that described for ODNs **VIa** and **VIb**. It should be noted that all couplings between amino-linked ODN **I–IV** and complex **7** resulted in the appearance of two product peaks in HPLC chromatograms (the resolution of these peaks in HPLC varied from 0.5 to 0.6 min for 5',3'-bis-ruthenated ODN and middle-ruthenated ODN up to 2.4 min for 5'-conjugated ODN), as shown in Figure S4. The PAGE showed (Figure 2C) they have similar mass-to-charge ratios, and it is concluded that these peaks represent the partially resolved mixtures of four possible diastereomers (for mono-metalated species), which result from (i) two possible orienta-

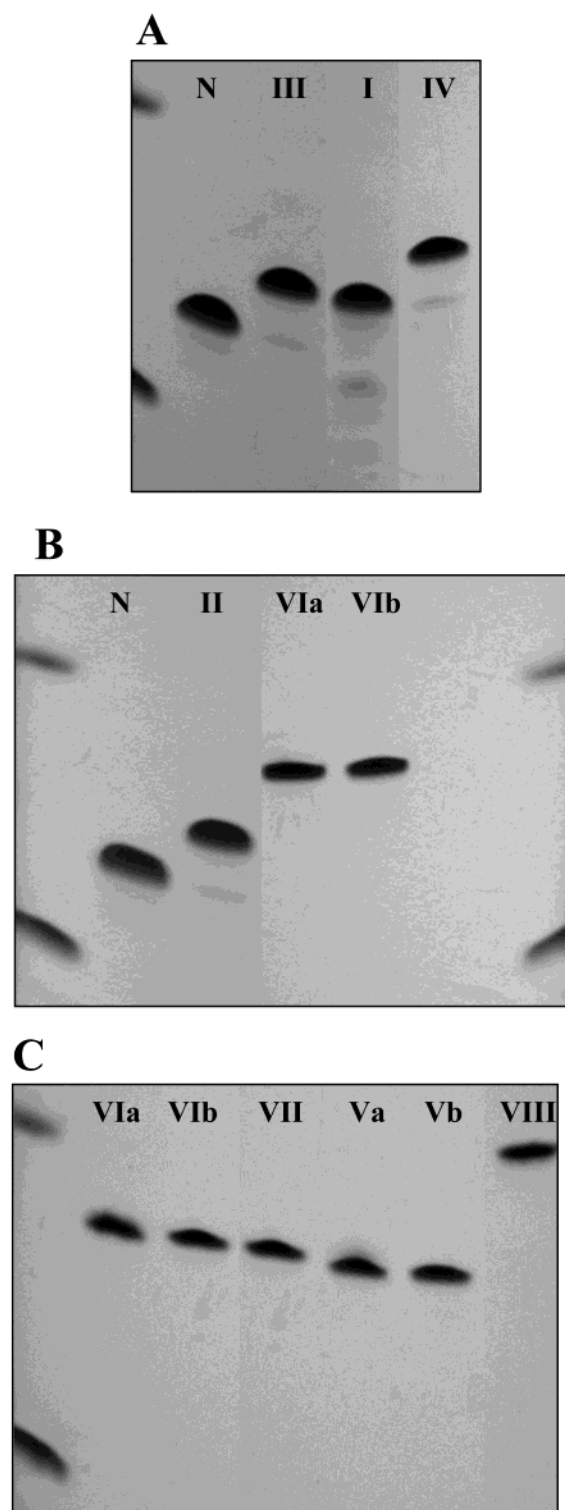


Figure 2. UV-shadowing PAGE ($\lambda = 254$ nm) of ODNs **I–VIII** (see Table 1 for abbreviations) and their native counterpart (**N**)*, showing their purities: (A) native ODN and amino-modified ODNs **III**, **I**, and **IV**; (B) native ODN **N**, amino-modified ODN **II**, and Ru^{2+} -labeled ODNs **VIa** and **VIb** (obtained by postsynthetic reaction of ODN **II** + **7**) and reversed-phase HPLC purification (see Figure S1); (C) Ru^{2+} -labeled ODNs **VIa** and **VIb** obtained by automated solid-phase synthesis starting with $[\text{Ru}(\text{tpy})(\text{dppz})\text{Cl}]^+$ -modified support and purified by reversed-phase HPLC (see Figure S4). ODNs **VII**, **Va**, **Vb**, and **VIII** have been synthesized postsynthetically through the amide bond formation between complex **7** and ODNs **III**, **I**, and **IV**, respectively (see Experimental Part for detail).

Table 2. Thermal Stability (T_m , °C) of (Ru²⁺-ODN)·DNA Duplexes^a (1:1 Mixture)

entries	duplex type ^b	T_m	ΔT_m^a	entries	duplex type ^b	T_m	ΔT_m^a	ΔT_m^b
1	N·T	33.0	-					
2	I·T	34.5	1.5	6	V·T	50.5	17.5	16.0
3	II·T	34.4	1.4	7	VI·T	41.4	8.4	7.0
4	III·T	24.0	-9.0	8	VII·T	48.3	5.3	24.3
5	IV·T	35.5	2.5	9	VIII·T	56.6	23.6	21.1

^a $\Delta T_m^a = T_m - T_m(\text{N}\cdot\text{T})$, $\Delta T_m^b = T_m - T_m$ (analogue containing only linker **L**). ^b See Table 1 for abbreviations.

tions^{9c} of the linker attached to the dppz ligand in the complex (as shown in Schemes 1 and 2) and from (ii) the *R* and *S* stereoisomers of the racemic *sn*-glycerol moiety of the linker. Consequently, bis-metalation gives rise to eight possible isomers of ODN **VIII**. Thus, it is not surprising that we could not achieve complete separation of all isomers for synthesized ODNs **V–VIII**. Further study on the DNA·DNA duplex stability and photoreactivity showed no difference between separated fractions (consisting of partially resolved diastomers) of ODNs **V–VIII**, which will be entirely characterized below as mixtures of all possible isomers.

(V) Characterization of Ru²⁺-ODN Conjugates by Electrospray Ionization Mass Spectrometry. The ODN conjugates **V–VIII** have been characterized by ESI mass spectrometry. The ESI in the negative mode of mono-metalated ODNs **V–VII** (MW 3916) and bis-metalated ODN **VIII** (MW 4886) showed a number of multiply charged ions, which, after deconvolution, revealed the expected ODN anions at m/z 3913 and 4881 corresponding to $[\text{M} - 3\text{H}^+]^-$ and $[\text{M} - 5\text{H}]^-$, respectively, as shown in Figure S5(A) for ODN **VI**. Electrospray ionization mass spectrometry (ESI-MS) analysis of the separated fractions for the 5'- and 3'-[Ru(tpy)(dppz)(CH₃CN)]²⁺-modified ODNs **V** and **VI** revealed the same m/z ratio: **Va**, 3912.8; **Vb**, 3913.4; **VIa**, 3912.5; **VIb**, 3913.8. Diastomers of the middle-modified ODN **VII** could not be separated by HPLC (Figure S4(E)) because they eluted as two ill-resolved major peaks; they were therefore pooled together, examined by ESI, and showed the m/z of 3913.3, which is consistent with their proposed structure. Thus, these ESI-MS data lead us to conclude that all metalated DNA conjugates have the CH₃CN ligand intact in the coordination sphere of their Ru²⁺ label. The separated pure fractions **VIa** and **VIb** of the 3'-[Ru(tpy)(dppz)(CH₃CN)]²⁺-ODN conjugate, obtained by the automated solid-phase synthesis (as in Scheme 2), had m/z 3913.7 and 3913.2, respectively, i.e. identical to those obtained by postsynthetic labeling (Scheme 1). This implies that the [Ru(tpy)(dppz)Cl]⁺ complex attached to the solid support is relatively stable during the solid-phase ODN assembly and can be converted to the thermally stable Ru²⁺-CH₃CN conjugate after ammonia deprotection at room temperature.

The negative ion MALDI-TOF of the mono-metalated ODNs showed the 1- ions (expected m/z 3872 for $[\text{M}[(\text{C}_{141}\text{H}_{166}\text{N}_{42}\text{O}_{66}\text{P}_{10}^{102}\text{Ru})^{2+}] - \text{M}[\text{CH}_3\text{CN} + 3\text{H}^+)]$ corresponding to the loss of CH₃CN moiety from the molecular ion (see Experimental Part and Figure S5(B) as an example): m/z 3872.6 for ODN **Va**, m/z 3871.9 for **Vb**, m/z 3872.5 for **VIa**, m/z 3871.8 for **VIb**, m/z 3872.1 for **VII**, and m/z 3872.5 for **VIII**. Similarly, laser ionization of the bis-Ru²⁺-modified ODN **VIII** led to the loss of two acetonitrile molecules affording the 1- charged ions with m/z of 4798.4: $[\text{M}[(\text{C}_{186}\text{H}_{208}\text{N}_{51}\text{O}_{74}\text{P}_{11}^{102}\text{Ru}_2)^{4+}] - \text{M}[2\text{CH}_3\text{CN} + 5\text{H}^+]]$. It is noteworthy that some minor amount of

molecular ions corresponding to the Ru²⁺-ODN conjugates with CH₃CN ligand were detectable by MALDI-TOF MS.

The addition of imidazole to the ODN sample analyzed by ESI-MS led to the decrease of intensity of the [Ru(tpy)(dppz)-(CH₃CN)]²⁺-ODN peak and an increase in the intensity of the naked Ru²⁺-ODN species (data not shown). This observation supports²² that coordinated acetonitrile undergoes base hydrolysis to acetamide, which is released very rapidly from the Ru²⁺ coordination center, since amides are poor π -acceptor ligands.³⁰ The above observations thus clearly fingerprint that our [Ru(tpy)(dppz)(CH₃CN)]²⁺-ODN conjugates **V–VIII** are indeed *thermally stable* and can be *activated by light* through the dissociation of the CH₃CN ligand, which suggests that CH₃CN ligand can be expected to be replaced by other potential coordinating species if they exist in the reaction mixture.

(VI) Thermal Stability of (Ru²⁺-ODN)-DNA Duplexes. The ODN·DNA duplexes were generated by hybridization of ODNs **I–VIII** with the 11mer ODN target (**T**) (Table 1) in a 1:1 ratio (1 μM of each strand in 20 mM phosphate buffer, pH 7.0, and 0.1 M NaCl). Thermal denaturation profiles of all duplexes exhibited a single, cooperative melting transition. The melting temperatures derived from these experiments are collected in Table 2, which leads to the following conclusions: (i) A low T_m increase for the duplexes **I·T**, **II·T**, and **IV·T** (entries 2, 3, and 5 in Table 2) suggests that the amino-linker **L** tethered at 3'- or 5'- or at both terminals of 10mer strand **N** does not have a great influence on the thermodynamic behavior of a double helix. (ii) Conversely, internucleotide insertion of linker **L** (Table 1) between two central dC residues, as in ODN **III**, makes the linker **L** bulge out in the duplex **III·T** in order to provide Watson-Crick base pairing for the central 2 \times (C·G). This strongly disrupts the helix, as is clearly seen from the drop in T_m for **III·T** ($\Delta T_m^a = -9.0$ °C, entry 4 in Table 2). (iii) Tethering of the [Ru(tpy)(dppz-CO)(NCCH₃)]²⁺ moiety to the amino linker of ODNs **I–IV** crucially changes the stability of the corresponding ODN·DNA duplexes. The reason for the large increase in T_m s (ΔT_m^a varies from 8.4 to 23.6 °C, Table 2) for all metalated duplexes (entries 6–9 in Table 2) can be presumably due to the intercalative interaction^{9m,29} through the dppz moiety in addition to electrostatic stabilization provided by dipositive Ru²⁺ complex. We, however, do not have any evidence to support either of them. (iv) The strength of duplex stabilization for various site-specific Ru²⁺ incorporations into ODN compared to the native counterpart **N·T** are as follows: 5',3'-bis-Ru²⁺ > 5'-Ru²⁺ > middle Ru²⁺ > 3'-Ru²⁺-modified duplex (Table 2). This trend was also found for [Ru(phen)₂(dppz)]²⁺ conjugation.^{5m} (v) Interestingly, a comparison of T_m s of (Ru²⁺-ODN)·DNA duplexes with T_m s of structurally related amino-linker modified duplexes allows us to estimate the stabilization effect (ΔT_m^b) inherent in the [Ru(tpy)(dppz)-

(30) Naal, Z.; Tfouni, E.; Benedetti, A. V. *Polyhedron* **1994**, *13*, 133.

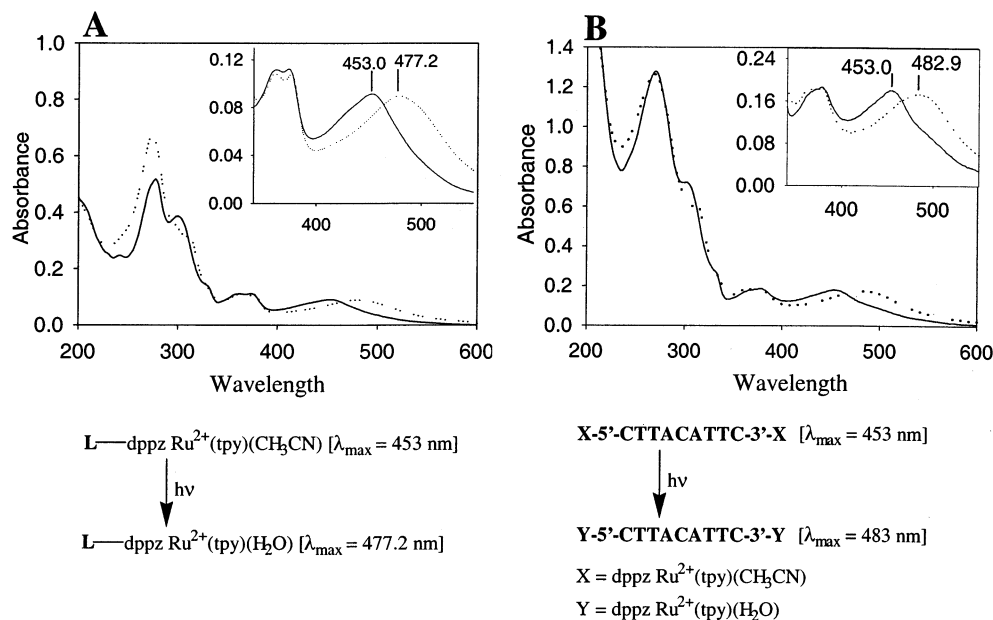


Figure 3. UV-vis absorption spectra of starting acetonitrile complex and their conversion to the aqua complex (note the difference in the maxima of their MLCT bands). (A) Aqueous solutions of $[\text{Ru}(\text{tpy})(\text{dppz}-\text{L})(\text{CH}_3\text{CN})](\text{PF}_6)_2$ (**17**, straight line) and $[\text{Ru}(\text{tpy})(\text{dppz}-\text{L})(\text{H}_2\text{O})](\text{PF}_6)_2$ (**18**, broken line), where **L** is a linker, $-\text{CONH}(\text{CH}_2\text{CH}_2\text{O})_2\text{CH}_2\text{CH}(\text{OH})\text{CH}_2\text{OH}$. Aquaruthenium complex **18** was obtained by irradiation (1 h) of corresponding $\text{Ru}^{2+}-\text{NCCH}_3$ analogue **17** as well as chemically from its $\text{Ru}^{2+}-\text{Cl}^-$ precursor **13** (see Experimental Part for details). (B) Aqueous solutions of ODN **VIII** (5.5×10^{-6} mol L^{-1}) before (straight line) and after (broken line) irradiation for 1 h.

$(\text{CH}_3\text{CN})]^{2+}$ complex itself (Table 2). Such an effect is most pronounced in the case of *internucleotide* conjugation (compare **III**·**T** with **VII**·**T**: $\Delta T_m^b = 24.3$ °C, entries 4 and 8 in Table 2) than for 5'-metalated ODN·DNA (1.5 times) or 3'-metalated duplexes (3.5 times).

(VII) Photodissociation of the CH_3CN Ligand from the Ru^{2+} Coordination Sphere of $[\text{Ru}(\text{tpy})(\text{dppz})(\text{CH}_3\text{CN})]^{2+}$ -ODNs. UV-Vis and Mass-Spectroscopic Evidence. The photochemical behavior of the ODNs **V**-**VIII** has been first examined in aqueous solution in the absence of any potential nucleophiles by UV-vis spectroscopy. Under light irradiation (1 h, $\lambda > 300$ nm) the MLCT absorption bands initially centered at 454 nm shifted to longer wavelength (482 nm), exhibiting three isobestic points in the 300–600 nm region (309, 387, and 465 nm, respectively) as demonstrated in Figure 3B and Figure S6 for ODNs **V**-**VIII**. A comparative study with **17** (Figure 3A) has been undertaken as a reference in order to establish photodissociation of the CH_3CN ligand in ODNs **V**-**VIII** in the course of light irradiation. Thus, complex **17** was photolyzed, and the product (Figure 3A), resulting from photosubstitution of CH_3CN ligand by water molecule, was identical (UV-vis and NMR) to authentic^{17b,27} $[\text{Ru}(\text{tpy})(\text{dppz}-\text{L})(\text{H}_2\text{O})](\text{PF}_6)_2$ (**18**; Scheme 2, Experimental Part), which was synthesized from **13** by treatment with silver *p*-toluenesulfonate in acetone-water (3:1, v/v).²⁷ Comparison of UV-vis in ODNs **V**-**VIII** with the monomeric Ru^{2+} complex **17** (Figures 3 and S6), as well as with their photolyzed products, leads us to conclude that an identical photosubstitution process takes place in $[\text{Ru}(\text{tpy})(\text{dppz})(\text{CH}_3\text{CN})]^{2+}$ -ODNs **V**-**VIII** to give the corresponding $[\text{Ru}(\text{tpy})(\text{dppz})(\text{H}_2\text{O})]^{2+}$ -ODN conjugates. The metalated ODNs were analyzed by PAGE before and after photolysis to confirm that no other degradation of the molecule occurs with the irradiation condition applied (Figure 4).

(VIII) Intermolecular Photochemical Cross-Linking of Monoaqua Ru^{2+} Complexes to the G-Rich Native DNA·DNA

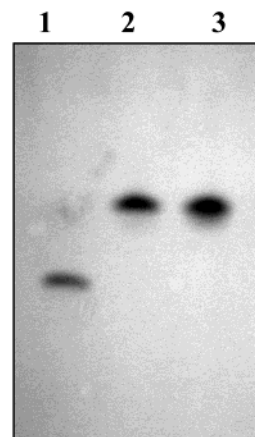


Figure 4. UV-shadowing PAGE ($\lambda = 254$ nm) of amino-modified ODN **III** (lane 1) and Ru^{2+} -labeled ODN **VII** before (lane 2) and after (lane 3) light irradiation for 1 h. Irradiation was performed in water at concentration of 10^{-5} mol L^{-1} under the same conditions applied for duplex photolysis (see Experimental Part).

Duplex. Thorp et al. first showed^{16a} that mono- and bis-aqua polypyridyl complexes of ruthenium(II) covalently bind to DNA, presumably at N7 of the G residue, with different efficiencies, depending upon the steric effects caused by polypyridyl ligands in octahedral geometry. Although an X-ray study³¹ of the complex of bis-aqua Ru^{2+} with 9-ethylguanine has recently confirmed N7 as the binding site of the G residue, *no* straightforward or any kind of spectroscopic evidence is however available supporting the structure of the complex of the mono-aqua complex with the G-base. We have therefore reinvestigated the reaction of mono-aqua ruthenium(II) complex generated in situ with a native DNA duplex to understand the molecular nature of this reaction in the Ru^{2+} -tethered ODN·DNA duplex.

(31) van Vliet, P. M.; Haasnoot, J. G.; Reedijk, J. *Inorg. Chem.* **1994**, *33*, 1934–1939.

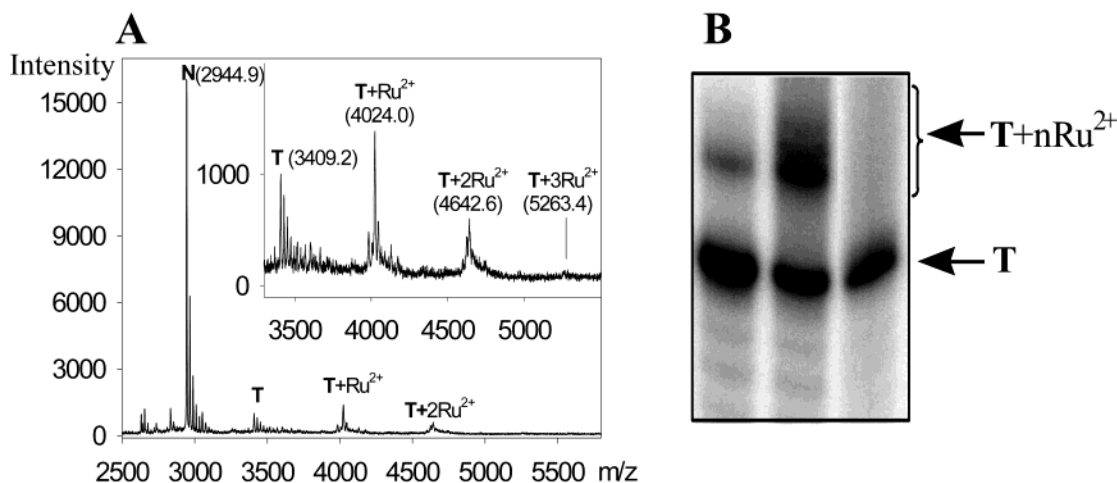


Figure 5. (A) Negative ion MALDI-TOF MS spectra of the native duplex $\text{N}\cdot\text{T}$ (10^{-5} mol L^{-1} ; reaction volume, 1600 μL) photolyzed with 5 equiv of $[\text{Ru}(\text{tpy})(\text{dppz})(\text{CH}_3\text{CN})]^{2+}$ for 2 h in 20 mM phosphate, pH 6.6, buffer and 0.1 M NaClO_4 and passed after photolysis through the Sephadex G-25 column to remove salts. The peaks corresponding to the target ODN T bound with $\text{Ru}^{2+}(\text{tpy})(\text{dppz})$ residues are depicted as $\text{T} + n\text{Ru}^{2+}$ ($n = 1, 2, 3$). (B) Autoradiogram of a 20% denaturing polyacrylamide gel of the photolyzed (2 h) complex $[\text{Ru}(\text{tpy})(\text{dppz})(\text{CH}_3\text{CN})]^{2+}$ and the duplex, $\text{N}\cdot\text{T}$ (formed with $5'$ - ^{32}P -labeled 11mer T and 10mer N) in 20 mM phosphate, pH 6.6, buffer and 0.1 M NaClO_4 . Lane 1: $[\text{Ru}(\text{tpy})(\text{dppz})(\text{CH}_3\text{CN})]^{2+}$ and duplex $\text{N}\cdot\text{T}$ in 1:1 ratio after photolysis. Lane 2: $[\text{Ru}(\text{tpy})(\text{dppz})(\text{CH}_3\text{CN})]^{2+}$ and duplex $\text{N}\cdot\text{T}$ in 5:1 ratio after photolysis. Lane 3: Pure $5'$ - ^{32}P -labeled 11mer T for comparison.

Thus, the photolysis of $[\text{Ru}(\text{tpy})(\text{dppz})(\text{CH}_3\text{CN})]^{2+}$ in the presence of the native duplex $\text{N}\cdot\text{T}$ (N is the natural antisense ODN containing only dA, dC, and T, and T is the target dG rich sequence, Table 1) was conducted to establish the ability of the photoactivated monofunctional Ru^{2+} complexes to bind to the double-stranded DNA. The MALDI-TOF MS spectra of the photolyzed mixture (Figure 5A) revealed that the 10mer N (calculated monoisotopic mass is 2945.5; the observed mass is 2944.9) remained completely unaltered (with the partial addition of Na^+ indicated by the appearance of $(+23n)$ satellite peaks, n is a number of Na^+ cations), while the target T strand containing dG nucleotides showed two new peaks at m/z of 4024.0 and 4642.6 (Figure 5A) in addition to the native T at m/z 3409.2. The peaks at m/z of 4024.0 and 4642.6 correspond to the molecular weight of the mono cross-linked product $[\text{T} + \text{Ru}^{2+}(\text{tpy})(\text{dppz})]$ and bis cross-linked product $[\text{T} + (2 \cdot \text{Ru}^{2+}(\text{tpy})(\text{dppz}))]$. It is of interest to note that only two Ru^{2+} complex molecules at most bind to the target T strand of the duplex $\text{N}\cdot\text{T}$ (a negligible amount of the tris-ruthenated target T was detected with m/z of 5263.4), most probably to two terminal guanine residues. The terminal G residues are more reactive than the central G residues because of the fact that they are easily accessible for the Ru^{2+} complex for cross-linking compared to the internal ones which are firmly paired with the complementary dC nucleotides in the core of a double helix. Consistent with the MS data, the autoradiography of the PAGE of the photolyzed reaction mixture of $[\text{Ru}(\text{tpy})(\text{dppz})(\text{CH}_3\text{CN})]^{2+}$ and native duplex $\text{N}\cdot\text{T}$, formed with ^{32}P -labeled T strand, showed the appearance of a series of bands migrated more slowly compared to the parent ^{32}P -labeled target T (Figure 5B). Thus, the present study clearly establish that $[\text{Ru}(\text{tpy})(\text{dppz})(\text{CH}_3\text{CN})]^{2+}$ and its derivatives, upon light activation, can bind to the N7 of the guanine moiety of the dG nucleotides of the double-stranded DNA.

(IX) Intramolecular Photochemical Cross-Linking of $\text{Ru}^{2+}(\text{CH}_3\text{CN})$ -ODNs to the Complementary Strand in the Duplex. From the above intermolecular cross-linking experiment, it is clear that when a monofunctional Ru^{2+} complex is tethered to an ODN strand in a ODN-DNA duplex, it should

also cross-link, upon photoactivation, with the complementary target strand (T) containing G residue(s) in the direct proximity of the appended Ru^{2+} center. This was indeed observed for our $([\text{Ru}(\text{tpy})(\text{dppz})(\text{CH}_3\text{CN})]^{2+} - \text{ODN}) \cdot \text{DNA}$ duplexes when subjected to light irradiation, thereby confirming the in situ generation of the reactive aquaruthenium-ODN conjugates. The target strand, T , was constructed in such a way that, in all Ru^{2+} -modified duplexes, the Ru^{2+} complex is in close steric proximity to the target G residue (Table 1). Figure 6A shows the autoradiogram from the photolysis experiments of the duplexes immediately analyzed after irradiation (2 h) by PAGE in denaturing conditions. All of the ODNs **V–VIII** produced a higher molecular weight band (**P**) under light exposure, indicating the formation of a cross-linked product. As expected, the highest yield (34%) was obtained with the ODN **VIII** carrying two reactive Ru^{2+} centers at both 3'- and 5'-ends (lane 2 in Figure 6A). For ODNs carrying only one Ru^{2+} complex, as in **V–VII**, the reactivity is found to decrease in the following order: 3'- Ru^{2+} ODN (**VI** $\cdot\text{T}$) (22%) > 5'- Ru^{2+} ODN (**V** $\cdot\text{T}$) (9%) > middle- Ru^{2+} ODN (**VII** $\cdot\text{T}$) (7%). Thus, the cross-coupling efficiency of the tethered Ru^{2+} complex and the stabilization effect (see ΔT_m^b in Table 2) follow a reverse order. This means that as the structural rigidity of a metallointercalation site in a duplex increases [3'- Ru^{2+} ODN (**VI** $\cdot\text{T}$) ($\Delta T_m^b = 7^\circ\text{C}$) < 5'- Ru^{2+} ODN (**V** $\cdot\text{T}$) ($\Delta T_m^b = 16^\circ\text{C}$) < middle- Ru^{2+} ODN (**VII** $\cdot\text{T}$) ($\Delta T_m^b = 24.3^\circ\text{C}$) (see Table 2)], the photochemical cross-linking yield decreases. Clearly, the intercalation of the Ru^{2+} complex through the helix in the middle- Ru^{2+} -modified duplex (**VII** $\cdot\text{T}$) gives a more rigidly packed structure, reducing the metal center flexibility, and consequently the accessibility of the target G residue by the aquaruthenium moiety becomes severely restricted, which results in a poor yield in the cross-coupling reaction. MALDI-TOF MS analysis of the irradiated 3'- Ru^{2+} -modified duplex **VI** $\cdot\text{T}$ (Figure 6B, for an example) confirmed the formation of the cross-linked product generating 1- charged ions at m/z 7282.1 (calculated m/z 7281.6), which corresponds to the sum of the m/z values observed for the nonreacted target strand T (3410.3) and singly Ru^{2+} -modified

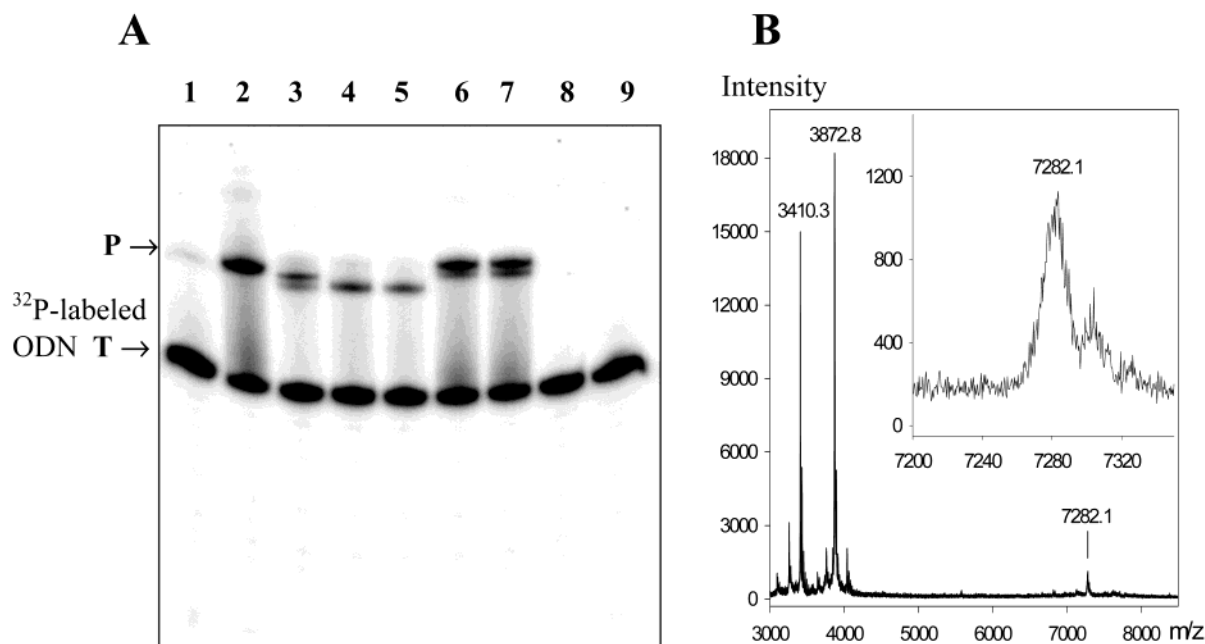


Figure 6. (A) Autoradiogram of a 20% denaturing polyacrylamide gel showing the interstrand photo cross-linked product (**P**) formed upon irradiation of duplexes formed with 5'-³²P-labeled 11mer **T** and Ru²⁺-labeled ODNs **V–VIII** in 20 mM phosphate, pH 6.6, buffer and 0.1 M NaClO₄. Lane 1: **VIII·T** without irradiation for reference. Lanes 2–7: The product (**P**) formed from the cross-linking of the Ru²⁺-labeled duplexes upon irradiation for 2 h. **VIII·T** (lane 2), **VII·T** (lane 3), **Va·T** (lane 4), **Vb·T** (lane 5), **VIIa·T** (lane 6), **VIIb·T** (lane 7), native **N·T** duplex for reference showing no product formation in the absence of tethered Ru²⁺ label (lane 8). Lane 9: 5'-³²P-labeled 11mer **T**. **Va** and **Vb** stand for two fractions for diastereomers obtained in the course of HPLC purification of ODN **V**. Corresponding two fractions of ODN **VI** are designated as **VIa** and **VIb** (see text for details). Duplex concentration = 10⁻⁵ mol L⁻¹. (B) Negative ion MALDI-TOF MS spectra of the Ru²⁺-labeled duplex **VI·T** (10⁻⁵ mol L⁻¹) irradiated for 2 h in 20 mM phosphate, pH 6.6, buffer and 0.1 M NaClO₄ and passed after photolysis through the Sephadex G-25 column to remove salts.

ODN **VI** with decoordinated CH₃CN ligand (3872.7, see Figure S5(B) for comparison).

(X) Kinetics of the Reaction of Tethered Monofunctional Ru²⁺ Complexes in the Duplex. The kinetics of photo cross-linking reaction for the 5',3'-bis-Ru²⁺-modified ODN with the target (**VIII·T**) was examined. It was photolyzed for 5 h, and aliquots were withdrawn at definite time intervals, immediately frozen, and lyophilized before PAGE analysis. The PAGE results are presented in Figure 7A (lanes 1–6). A plot of the percent yield as a function of time (Figure 7B) shows the yield of the adduct with ODN **VIII** is almost steady after 1 h of irradiation, achieving the *maximal value* of ~33% at the plateau. The reason for such a low saturation level of the cross-coupling reaction (as shown in Figure 7B) can be 2-fold: (i) the cross-coupling reaction is reversible because of low product stability, or (ii) the target reaction is accompanied by side reactions deactivating the intermediate aquaruthenium(II)–ODN conjugate. To examine the stability of the cross-coupling product, the reaction mixture obtained after irradiation for 5 h was kept at room temperature and analyzed by PAGE (Figure 7A, lanes 7–9). It can be seen that the yield of the high molecular weight cross-linked product (**P** in Figure 7A) relative to the starting ³²P-labeled target ODN **T** very slowly decreases from 33% to 25% over a period of standing at room temperature for 15 h. When the ³²P-labeled high molecular weight band (i.e. low-migrating **P** band on PAGE in Figure 7A, lane 5) was excised, and extracted from the gel with sodium acetate (0.3 M), the analytical PAGE of the isolated cross-coupled product revealed ca. 50% regeneration of the nonmodified ³²P-labeled target ODN **T** (Figure 7C, lane 2). This shows that the photo cross-coupling of the double strands is a slow reversible reaction, which *under*

the present reaction condition gives an yield of ca. 25% of the photoadduct for the bis-Ru²⁺-modified duplex (lane 9 in Figure 7A).

We have subsequently performed the photo cross-linking reaction in a large scale (with 17 nmol of duplex compared to the analytical photolysis experiments (0.2 nmol) with ³²P-labeled target ODN **T**) for the 3'-Ru²⁺-modified duplex **VI·T** and 5',3'-bis-Ru²⁺-modified duplex **VIII·T** in order to examine if any other product is formed during the reversible reaction: The reaction mixtures were desalted and then separated by PAGE and were examined both under 254 and 366 nm lamps (Figure 8A). Optimal separation of the photoproduct (from **VI·T**) was achieved in the case of the mono-Ru²⁺-labeled duplex (lane 1 in Figure 8A). UV-shadowing PAGE at 366 nm for the photo cross-linking experiment with **VI·T** clearly exhibits that the photoproduct (*low-migrated band*) contains Ru²⁺ complex. The low-migrated band in PAGE (lane 1 in Figure 8A) was excised and examined by MALDI-TOF MS (Figure 8B). The fragmentation pattern in MALDI-TOF MS showed the presence of both product and starting materials (**VI** and **T**). This showed that the adduct is partially unstable to give starting materials (**VI** and **T**) without any secondary modifications. On the other hand, the fluorescent photoproduct band (visible at 366 nm) in the reaction of bis-Ru²⁺-modified duplex (**VIII·T**) has electrophoretic mobility very similar to that of the parent ODN **VIII**, but free of target **T** (lane 2 in Figure 8A), and they could not be separated. The low-migrated product band with ODN **VIII** in PAGE (lane 2 in Figure 8A) was excised and examined by MALDI-TOF MS (Figure 8C), which showed peaks for both starting materials (**VIII** and **T**) as well as the photoproduct (*m/z* 8206.7). The product peak at *m/z* 8206.7 most probably

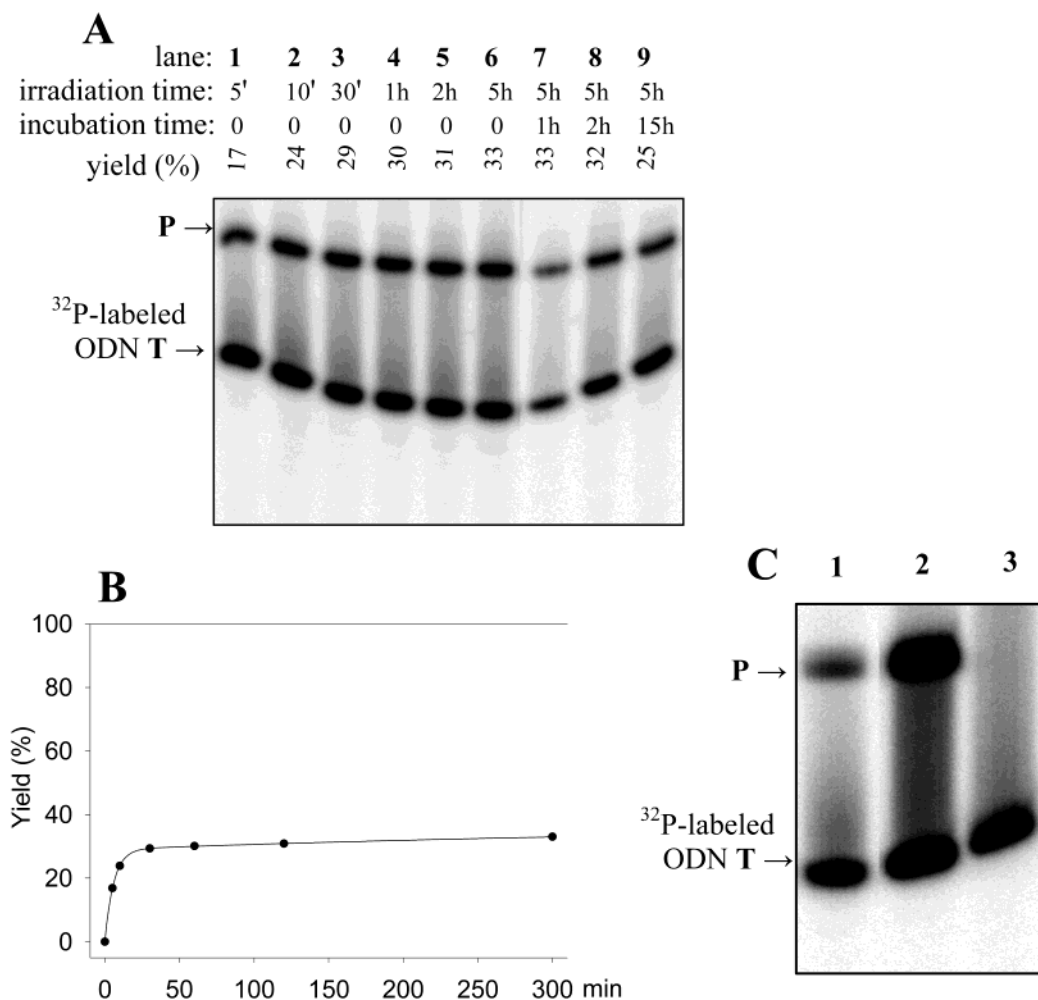


Figure 7. (A) Autoradiogram of a 20% denaturing polyacrylamide gel showing the photo cross-linked duplex (**P**) formed with 5'-³²P-labeled 11mer **T** and 5',3'-bis-Ru²⁺-labeled ODN **VIII** in 20 mM phosphate, pH 6.6, buffer and 0.1 M NaClO₄. Lanes 1–6: duplex **VIII**·**T** irradiated at room temperature for 5 min, 10 min, 30 min, 1 h, 2 h, or 5 h, and immediately analyzed by PAGE after photolysis. Lanes 7–9: duplex **VIII**·**T** irradiated for 5 h at room temperature, which is then kept standing at room temperature (without photoirradiation) for 1, 2, or 15 h, respectively, showing the yield of the cross-linked photoadduct is ca. 25% (after 15 h). (B) Plot of cross-coupling product (**P**) yield versus irradiation time for duplex **VIII**·**T** immediately analyzed by PAGE after photolysis experiments, showing a maximum yield of 33% for cross-linked product, **P**, at the plateau. The duplex concentration in each experiment was 10⁻⁵ mol L⁻¹. (C) Autoradiogram of a 20% denaturing polyacrylamide gel showing the high molecular weight band (**P**) after photolysis (2 h) of the duplex formed with 5'-³²P-labeled 11mer **T** and 5',3'-bis-Ru²⁺-labeled ODN **VIII** in 20 mM phosphate, pH 6.6, buffer and 0.1 M NaClO₄ (lane 1), followed by excision of the high molecular weight band (i.e. **P**), extraction from the gel with sodium acetate (0.3 M) overnight at room temperature, and passing through the Sephadex G-25 column (lane 2), showing **P** and 5'-³²P-labeled 11mer **T** in ca. 1:1 ratio. Lane 3: 5'-³²P-labeled 11mer **T**.

coprresponds to a mixture of two mono (3'-Ru²⁺-G and 5'-Ru²⁺-G) adducts as well as the bis-adduct. Clearly, it is not possible to distinguish the composition of this mixture from mass spectrometry (Figure 8C) since both mono- or/and bis-cross-linked products have the same mass.

To confirm the reversibility of binding of the monofunctional polypyridyl Ru²⁺ complexes, [Ru(tpy)(dppz-CONHEt)(H₂O)]²⁺ was reacted to 5'-dGMP in equimolar ratio in an acetone-*d*₆/D₂O mixture at various temperatures; the time dependence of the reaction was monitored by ¹H NMR. The composition of this reaction mixture was identified by positive ion mode MALDI-TOF MS as a mixture of the starting complex **9**, which is ionized with the loss of a H₂O molecule [Ru²⁺(tpy)(dppz-CONHEt)-H⁺], the calculated monoisotopic mass is 687 and the observed mass is 687.1, and the product, (dppz-CONHEt)(tpy)Ru²⁺-dGMP (*m/z* = 1034). The overall composition of the product peak (1034) fits the expected adduct of the formula [C₄₆H₃₉N₁₃O₈PRu]⁺, indicating that complex **9** covalently binds to dGMP in the course of incubation. The observed kinetics

(Figure 9A) showed that the reaction never goes to completion and, in fact, reaches an equilibrium depending upon the reaction condition. Data points (concentration as a function of time) have been approximated with functions derived from the rate law equation for a reversible reaction of the type A + B ⇌ X + Y, and equilibrium constants *K* (1.87 × 10⁴ to 1.07 × 10⁵ for the temperature range of 56–20 °C) were obtained from the extrapolation of such functions to infinite time (see Experimental Part for details). As seen from experimental data, the equilibrium is only slightly shifted to the product side with the decrease of temperature, which indicates that the reaction is poorly exothermic. Fitting of observed equilibrium constants *K* to the Van-Hoff equation (Figure 9B) gave -39.3 ± 1.7 kJ/mol for Δ*H*^o and -0.038 ± 0.006 kJ/(mol K) for Δ*S*^o (-*T*Δ*S*^o = 11.0 ± 1.7 kJ/mol). Our experimental results show that the product complex, [Ru(tpy)(dppz-CONHEt)(dGMP)], thus formed suffers a slow reverse aquation and exists in equilibrium with [Ru(tpy)(dppz-CONHEt)(H₂O)]²⁺, in 8:2 ratio in favor of the adduct, at room temperature (Figure 9A). Next, we added an

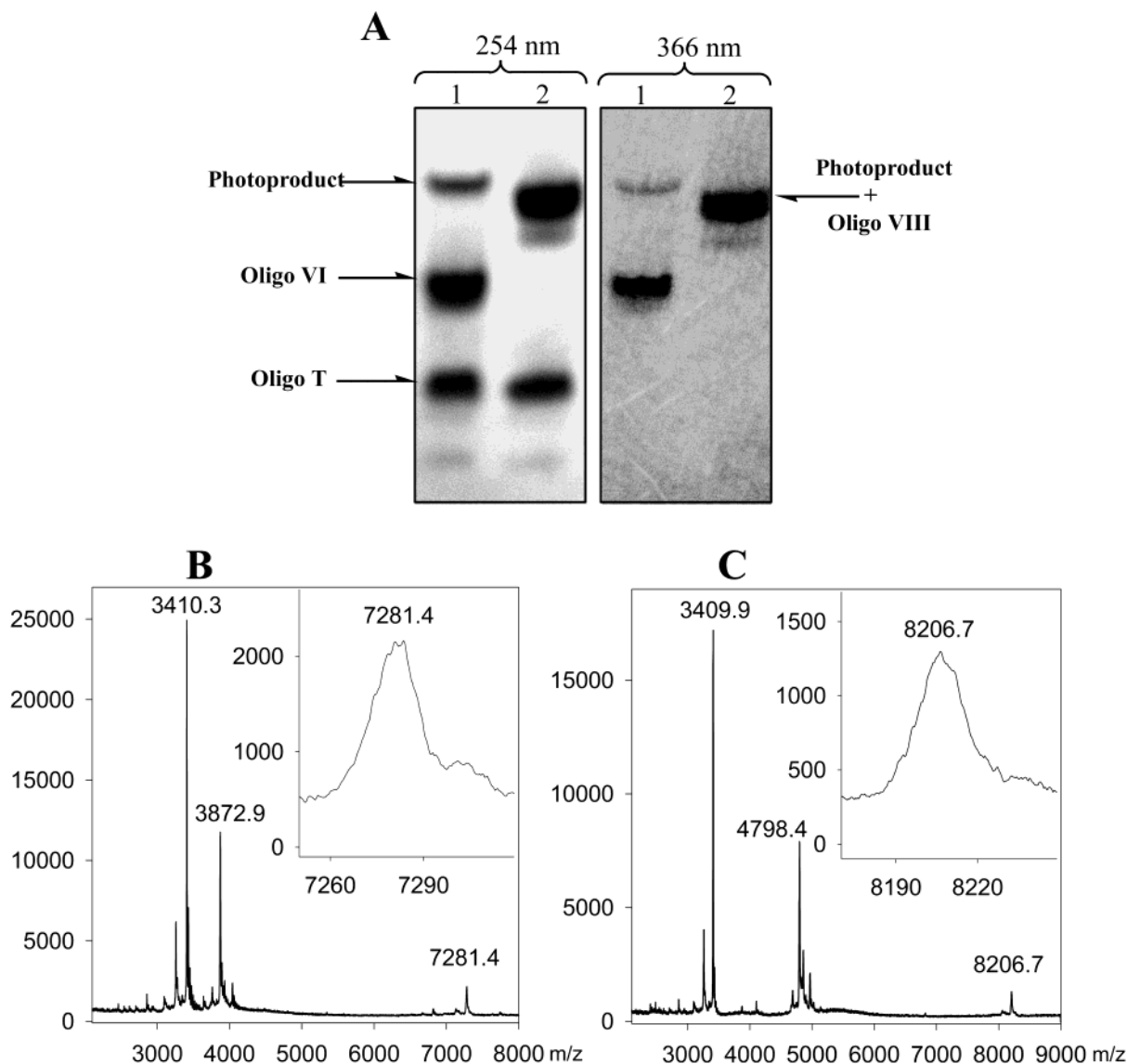


Figure 8. (A) UV-shading 20% denaturing polyacrylamide gel at $\lambda = 254$ (left) and 366 nm (right) of the reaction mixtures obtained after photolysis of 3'-Ru²⁺-labeled duplex T·VI (lane 1) and 5',3'-bis-Ru²⁺-labeled duplex T·VIII (lane 2) in 20 mM phosphate, pH 6.6, buffer and 0.1 M NaClO₄ (duplex concentration in each experiment was 10⁻⁵ mol L⁻¹; reaction volume, 1600 μ L) after the reaction mixtures are passed through the Sephadex G-25 column to remove salts. Comparison of the bands visualized at 254 and 366 nm show that the low-migrated bands (i.e. high molecular photoproduct) indeed show fluorescence at 366 nm, which indicates that the photoproduct consists of Ru²⁺ cross-linking. The low-migrated photoproduct bands in each lane were excised and then extracted from the gel with sodium acetate (0.3 M). The extracts were passed through the Sephadex G-25 column and analyzed by negative ion MALDI-TOF MS, shown in B and C. The peaks at m/z 7281.4 and 8206.7 correspond to the molecular weight of the photo cross-coupled Ru²⁺ containing duplexes.

excess of CH₃CN to the reaction mixture when it has already reached the equilibrium, and incubated in the dark at room temperature. After 17 h of incubation with CH₃CN, ¹H NMR spectra indicated only (data not shown) the presence of starting dGMP and [Ru(tpy)(dppz-CONHET)(CH₃CN)](PF₆)₂ (**8**), which finally confirms the reversibility of the reaction. Relatively poor stability of the adduct could be a consequence of high distortions of octahedral geometry which arise to minimize steric constraints between bulky guanine and polypyridyl ligands (tpy and dppz).

Conclusions

(1) The monofunctional [Ru(tpy)(dppz)(CH₃CN)]²⁺ complex has been attached to oligodeoxynucleotide by postsynthetic labeling of the appropriate amino-linker modified ODN precursors as well as by automated solid-phase synthesis on a support labeled with the [Ru(tpy)(dppz)Cl]⁺ complex.

(2) The conjugates prepared by both synthetic strategies were characterized by ultraviolet-visible absorption spectroscopy, enzymatic digestion, polyacrylamide gel electrophoresis, and mass spectrometry.

(3) The 5', 3', middle-, and 5',3'-bis-Ru²⁺-modified ODNs form duplexes with 11mer DNA target, which are significantly stabilized ($\Delta T_m = 8.4$ –23.6 °C) compared with the natural DNA·DNA duplex.

(4) The [Ru(tpy)(dppz)(CH₃CN)]²⁺-ODN conjugates undergo CH₃CN ligand decoordination under light irradiation with subsequent photoaquation of the appending Ru²⁺ complex producing reactive [Ru(tpy)(dppz)(H₂O)]²⁺-ODN intermediates in pure aqueous solutions.

(5) When [Ru(tpy)(dppz)(CH₃CN)]²⁺-ODNs are hybridized with the DNA target, containing dG nucleotides in the close

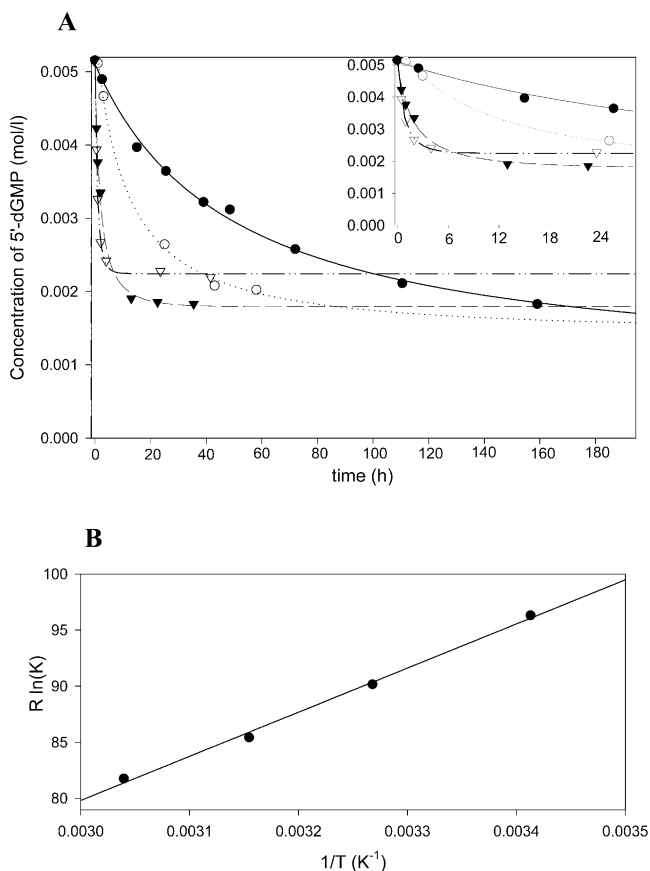


Figure 9. (A) Kinetic study of the 1:1 reaction between Ru²⁺ metal complex **9** and 5'-dGMP in CD₃COCD₃-D₂O (1:1, v/v) solution at 20 (●), 33 (○), 44 (▼), and 56 °C (▽), which show that the yield of the photoadduct varies from 80 to 60% in the temperature range of 20–56 °C. (B) Plot of $R \ln K$ vs $1/T$ obtained from the corresponding kinetic studies, giving the enthalpy ΔH° and entropy ΔS° from the slope and intercept, respectively: $R \ln K = \Delta S^\circ - \Delta H^\circ(1/T)$.

proximity of the Ru²⁺ label, the illumination leads to the formation of a cross-link between the metalcomplex tether and the G base. The complexation of the guanine derivative to the polypyridyl Ru²⁺(tpy)(dppz) moiety generating in the course of CH₃CN ligand photoexclusion finally affords the adduct in which most probably the guanine ring suffers strong steric repulsions from the other polypyridyl rings. This makes the resulting octahedral Ru²⁺ system very congested and relatively unstable. Contrary, small entering ligands with less ability to induce steric repulsions (as in the [Ru(tpy)(dppz)(py)]²⁺ analogue, py = pyridine) can form stable adducts with Ru²⁺(tpy)(dppz) species.

Implication. In contrast to the agents which bind to DNA on the basis of their chemical reactivities (for example, bromoacetyl,³² nitrogen mustard³³ residues, *cis*-chloroplatin,³⁴ aziridine³⁵), photochemical counterparts^{9i,36} (psoralens,³⁷ porphyrins,³⁸ *p*-azidophenacyl,³⁹ 3-azidoflavine⁴⁰) have an advantage that such chemicals can be selectively activated both in time and space to interstrand cross-link or oxidize, thereby

minimizing the toxic side effects within healthy tissue. On the other hand, real regulation of gene expression can however be only achieved by precise directing the drug reactivity to the desired DNA or RNA sequence through the attachment of the reactive moiety to the oligonucleotide, which hybridizes to the target nucleic acid in a sequence specific manner. This is the first report of Ru²⁺-labeled ODNs which can be easily synthesized and are thermally stable. They can be targeted to complementary DNA to form a duplex, and subsequently activated by light, owing to the photoaquation of their Ru²⁺ label, and then cross-link two DNA strands of the duplex. Thus, these Ru²⁺-labeled ODNs provide a “switch-like” mechanism that permits the metal complex to be turned on after duplex formation. By varying the number of coordination sites available for photoaquation in octahedral polypyridyl Ru²⁺ complexes or the type of entering ligands one can highly control both the reactivity and specificity of the resulting aquaruthenium(II)-ODN conjugates.

Experimental Part

(I) Materials. The complexes Ru(tpy)Cl₃,⁴¹ [Ru(tpy)(dppz)(X)](PF₆)_n (X = Cl⁻, H₂O, or CH₃CN)^{17b,22c} were prepared according to literature procedures. Compounds **1**, **9**, **10**, and dipyrido[3,2-*a*:2',3'-*c*]phenazine-11-carboxylic acid were synthesized according to ref 24. Dry pyridine was obtained by distillation over 4-toluenesulfonyl chloride. Acetonitrile and dichloromethane were distilled from P₂O₅ under argon. Dimethylformamide was distilled over CaH₂. Acetone was dried with anhydrous K₂CO₃ and then distilled. The silica gel Merck G60 was used for column chromatographic separations of all the protected intermediates. Thin layer chromatography (TLC) was performed on precoated silica gel F₂₅₄ plates with fluorescent indicator in the following mixtures: dichloromethane-ethanol (90:10, v/v) (A) and (80:20, v/v) (B), cyclohexanes-ethyl acetate (50:50, v/v) (C), acetonitrile-water-aqueous saturated KNO₃ (100:10:1, v/v/v) (D). ¹H NMR spectra (δ scale; J values are in Hz) were obtained at 270 MHz on a JNM-GX 270 spectrometer with SiMe₄ as an internal standard. ³¹P NMR spectra were obtained at 36 MHz on the same spectrometer using 85% phosphoric acid as external standard. ¹³C NMR spectra were obtained at 22.5 and 69 MHz in the same solvent using the solvent resonance as the internal standard.

11-[(9-Fluorenylmethoxycarbonyl)amino]-1-[(4,4'-dimethoxytriptyloxy)methyl]-3,6,9-trioxundecan-1-ol (2). 9-Fluorenylmethyl chloroformate (168 mg, 0.65 mmol) was added to a stirring solution of compound **1** (284 mg, 0.54 mmol) and *N,N*-diisopropylethylamine (110 μ L, 0.65 mmol) in dry DMF (1.5 mL). The mixture was stirred 1 h at room temperature and then poured into cold saturated NaHCO₃ (10 mL) to precipitate the product. The solid was collected by filtration and washed several times with water. The precipitate was taken up in CH₂Cl₂-cyclohexane (1:1) and purified by silica gel column chromatography eluting first with 50–100% CH₂Cl₂ in cyclohexane and then with 0–4% EtOH in CH₂Cl₂ (270 mg, 67% yield). R_f : 0.56 (A). ¹H NMR (CDCl₃): 7.75 (2H, d, Fmoc, J = 7.4), 7.58 (2H, d, Fmoc, J = 7.4), 7.41–7.14 (13H, m, Fmoc and DMT), 6.77 (4H, d, DMT, J =

(32) Povsic, T. J.; Strobel, S. A.; Dervan, P. B. *J. Am. Chem. Soc.* **1992**, *114*, 5934–5941.
 (33) Kutayavin, I. V.; Gamper, H. B.; Gall, A. A.; Meyer, R. B. *J. Am. Chem. Soc.* **1993**, *115*, 9303–9304.
 (34) (a) Vlassov, V. V.; Gorn, V. V.; Ivanova, E. M.; Kazakov, S. A.; Mamaev, S. V. *FEBS Lett.* **1983**, *162*, 286. (b) Gruff, E. S.; Orgel, L. E. *Nucleic Acids Res.* **1991**, *19*, 6849. (c) Berghoff, U.; Schmidt, K.; Janik, M.; Schröder, G.; Lippert, B. *Inorg. Chim. Acta* **1998**, *269*, 135.

(35) Reed, M. W.; Wald, A.; Meyer, R. B. *J. Am. Chem. Soc.* **1998**, *120*, 9729.
 (36) (a) Bendinskas, K. G.; Harsch, A.; Wilson, R. M.; Midden, W. R. *Bioconjugate Chem.* **1998**, *9*, 555–563. (b) Kobertz, W. R.; Essigmann, J. M. *J. Am. Chem. Soc.* **1997**, *119*, 5960–5961.
 (37) Giovannangeli, C.; Thoung, N. T.; Hélène, C. *Nucleic Acids Res.* **1992**, *20*, 4275.
 (38) Sessler, J. L.; Sansom, P. I.; Kral, V.; O'Connor, D.; Iverson, B. L. *J. Am. Chem. Soc.* **1996**, *118*, 12322–12330.
 (39) Praseuth, D.; Perrouault, L.; Doan, T. L.; Chassignol, M.; Thoung, N. T.; Hélène, C. *Proc. Natl. Acad. Sci. U.S.A.* **1988**, *85*, 1349–1353.
 (40) Doan, T. L.; Perrouault, L.; Praseuth, D.; Decout, J.-L.; Habhou, N.; Lhomme, J.; Thoung, N. T.; Hélène, C. *Nucleic Acids Res.* **1987**, *15*, 7749–7760.
 (41) Sullivan, B. P.; Calvert, J. M.; Meyer, T. J. *Inorg. Chem.* **1980**, *19*, 1404.

8.9), 5.94 (1H, t, NH, $J = 5.2$), 4.32 (2H, d, CH₂ of Fmoc, $J = 7.1$), 4.14 (1H, t, CH of Fmoc, $J = 7.1$), 4.08–3.93 (1H, m, DMTOCH₂CH), 3.74 (6H, s, 2 OCH₃), 3.69–3.50 (12H, overlapping m), 3.40–3.35 (2H, m, NHCH₂), 3.23–3.11 (2H, m, DMTOCH₂).

{11-[(9-Fluorenylmethoxycarbonyl)amino]-1-[[4,4'-dimethoxytrityl]oxy]methyl}-3,6,9-trioxoundecan-1-yl]-2-cyanoethyl-*N,N*-diisopropylphosphoramidite (3). Compound **2** (142 mg, 0.19 mmol, dried overnight at high vacuum) and *N,N*-diisopropylethylamine (0.17 mL, 0.95 mmol) were dissolved in dry CH₂Cl₂ under nitrogen. 2-Cyanoethyl diisopropylphosphoramidochloridite (90 mg, 0.38 mmol) was added, and the solution was stirred for 1 h at room temperature. The reaction mixture was worked up with aqueous saturated NaHCO₃ and dried over MgSO₄, coevaporated with toluene, and then with CH₂-Cl₂ to afford the gummy residue. The crude product was isolated by silica gel column chromatography, eluting with ethyl acetate–cyclohexane–Et₃N (50:50:2, v/v/v). Eluted fractions were evaporated, redissolved in a minimum of CH₂Cl₂ and precipitated with cold hexane. The precipitate was separated by ultracentrifugation and thoroughly dried under vacuum to give a white foam (138 mg, 77%). R_f : 0.48 and 0.53 (C) for two spots corresponding to product diastereomers. ³¹P NMR (CDCl₃): 147.9, 148.2.

{11-[(9-Fluorenylmethoxycarbonyl)amino]-1-[[4,4'-dimethoxytrityl]oxy]methyl}-3,6,9-trioxoundecan-1-yl]succinate (4) and Its Attachment to CPG. Compound **2** (85 mg, 0.114 mmol) and 4-(dimethylamino)pyridine (59 mg, 0.48 mmol) were dissolved in dry CH₂Cl₂ (1.8 mL). Then, succinic anhydride (46 mg, 0.46 mmol) was added, and the solution was stirred at room temperature for 5 h. The reaction mixture was first extracted with 0.1 M citric acid followed by aqueous saturated NaHCO₃ solution. The organic phase was dried over MgSO₄ and evaporated. The crude product was purified by silica gel column chromatography eluting with 0–20% EtOH in CH₂Cl₂. Yield: 63 mg, 65%. R_f : 0.48 (A). ¹H NMR (CDCl₃): 7.75 (2H, d, Fmoc, $J = 7.4$), 7.60 (2H, d, Fmoc, $J = 7.4$), 7.41–7.16 (13H, m, Fmoc and DMT), 6.80 (4H, d, DMT, $J = 8.7$), 5.67 (1H, t, NH, $J = 5.2$), 5.24 (1H, m, DMTOCH₂CH), 4.38 (2H, d, CH₂ of Fmoc, $J = 7.2$), 4.21 (1H, t, CH of Fmoc, $J = 7.2$), 3.77 (6H, s, 2-OCH₃), 3.67–3.56 (12H, overlapping m), 3.41–3.37 (2H, m, NHCH₂), 3.20 (2H, d, DMTOCH₂, $J = 5.2$), 2.64 (4H, m, CH₂CH₂ of succinyl).

To a solution of **4** (62.5 mg, 74 μmol) in dry acetonitrile (5 mL) was added 370 mg of aminopropyl CPG, *N,N*-diisopropylethylamine (1.2 mL, 7.4 mmol), benzotriazol-1-yloxytris(dimethylamino)phosphonium hexafluorophosphate (65 mg, 148 μmol), and *N*-hydroxybenzotriazole (20 mg, 148 μmol). The mixture was gently agitated at room temperature for 2 h; the CPG was filtered, washed (CH₂Cl₂), and assayed for loading of **4** (49 μmol/g resin). The excess of amino groups on the support was then acetylated with 3.3 mL of acetic anhydride–pyridine (9:91, v/v) containing 4-(dimethylamino)pyridine (59 mg) for 2 h. The support was then filtered and thoroughly washed with pyridine, CH₂Cl₂ (4 times), and diethyl ether (4 times) and then vacuum-dried.

[Ru(tpy)(dppz–COOH)Cl]Cl (5). Ru(tpy)Cl₃ (704 mg, 1.6 mmol) and dipyrido[3,2-*a*:2',3'-*c*]phenazin-11-carboxylic acid (522 mg, 1.6 mmol) were heated at reflux for 4 h in 140 mL of EtOH–H₂O (3:1, v/v) containing LiCl (374 mg, 8.8 mmol) and Et₃N (0.4 mL) as a reductant. The pot contents were filtered hot, and their volume was reduced to ~40 mL with a rotary evaporator. The chloride salt of product was precipitated by the addition of acetone (280 mL) and cooling (4 °C) for 2 h. The solid was filtered onto a fine-porosity frit, rinsed with acetone and diethyl ether, and air-dried (724 mg, 62% yield). R_f : 0.05 (D). ¹H NMR (CD₃OD): 10.60 (1H, d, H_a, $J = 5.4$), 9.91 (1H, m, H_c), 9.32–9.30 (1H, m, H_d), 8.89 (1H, m, H_e), 8.81 (2H, d, H₅ and H₇, $J = 8.2$), 8.66 (2H, d, H₄ and H₈, $J = 7.9$), 8.60–8.53 (2H, m, H_b and H_h), 8.44–8.35 (1H, m, H_i), 8.33 (1H, t, H₆, $J = 8.2$), 8.02 (2H, t, H₃ and H₉, $J = 7.7$), 7.91–7.87 (3H, m, H_f, H₁, H₁₁), 7.56 (1H, t, H_e, $J = 6.2$), 7.36 (2H, t, H₂ and H₁₀, $J = 6.9$).

[Ru(tpy)(dppz–COOH)(CH₃CN)]Cl (6). Compound **5** (265 mg, 0.36 mmol) was refluxed in 125 mL of CH₃CN–H₂O (1:1, v/v) in the

dark for 4 h under nitrogen. Reaction volume was then reduced to ~60 mL and filtered. The red solution was evaporated to dryness (278 mg, 100% yield) and kept protected from light. R_f : 0 (D). ¹H NMR (D₂O–CD₃OD, 7:4, v/v): 10.16–10.10 (1H, m, H_a), 8.88 (2H, d, H₅ and H₇, $J = 8.2$), 8.75 (2H, d, H₄ and H₈, $J = 8.2$), 8.69–8.52 (3H, m, H_c, H_g, H₆), 8.34–8.19 (3H, m, H₃, H₉, H_b), 8.07 (2H, d, H₁ and H₁₁, $J = 5.2$), 7.98, 7.87 (2H, 2d, H_d, H_f), 7.68–7.50 (3H, m, H₂ and H₁₀, H_h), 7.31–7.28 (1H, m, H_i), 7.08–7.03 (1H, m, H_e), 2.42 (3H, s, CH₃CN).

Activated Ruthenium Complex 7 (Cl[−] Salt). *N,N,N',N'*-Tetramethyl(succinimido)uronium tetrafluoroborate (19.5 mg, 65 μmol) and *N,N*-diisopropylethylamine (14 μL, 81 μmol) were added to a solution of **6** (42 mg, 54 μmol) in dry DMF (2.7 mL) under exclusion of moisture. The mixture was stirred in the dark at room temperature for 2 h under nitrogen. The product was precipitated by the addition of diethyl ether (10 mL). The solid was filtered onto a fine-porosity frit, washed several times with diethyl ether, and vacuum-dried to give **7** (44 mg, 93%), which was directly used for the coupling with amino-modified ODNs. R_f : 0.20 (D). ¹H NMR (CD₃OD): 10.32, 10.27 (1H, 2d, H_a, $J = 5.5$), 10.10, 9.93 (1H, 2d, H_c, $J = 8.4$), 9.59, 9.40 (1H, 2d, H_d, $J = 7.7$), 8.89 (1H, m, H_g), 9.27, 8.93 (1H, 2s, H_e), 8.97 (2H, d, H₅ and H₇, $J = 8.2$), 8.81–8.56 (6H, m, H₄, H₈, H_b, 2H_h, H₆), 8.22–8.14 (2H, m, H₃ and H₉), 8.04–7.95 (3H, m, H_f, H₁, H₁₁), 8.22–8.14 (1H, m, H_e), 7.54–7.44 (2H, m, H₂ and H₁₀).

[Ru(tpy)(dppz–CONHEt)(CH₃CN)](PF₆)₂ (8). NHS ester **7** (82.5 mg, 95 μmol) was dissolved in 1.2 mL of dry DMF. A 33% ethanolic solution of ethylamine (28 μL, 158.5 μmol of C₂H₅NH₂) was added; the mixture was stirred under nitrogen for 2 h and then concentrated. The residue dissolved in a minimum amount of ethanol was added to a solution of deionized water saturated with NH₄PF₆. The resulting suspension was partitioned between CH₂Cl₂ and aqueous NaHCO₃. The aqueous phase was extracted with CH₂Cl₂ (three times), and all combined organic phases were then dried over MgSO₄ and evaporated. The crude material was silica gel chromatographed (0–20% EtOH in CH₂Cl₂) to give red crystals (76 mg, 79%). R_f : 0.64 (B). ¹H NMR (acetone-*d*₆): 10.48 (1H, d, H_a, $J = 5.4$), 10.13 (1H, d, H_c, $J = 8.4$), 9.64 (1H, d, H_d, $J = 8.2$), 9.09 (1H, d, H_g, $J = 1.5$), 9.05 (2H, d, H₅ and H₇, $J = 8.2$), 8.88 (2H, d, H₄ and H₈, $J = 8.2$), 8.78–8.56 (4H, m, H_b, H₆, 2H_h), 8.35 (1H, t, NH, $J = 5.2$), 8.29–8.23 (3H, m, H₃, H₉, H_f), 8.14 (2H, d, H₁ and H₁₁, $J = 5.4$), 7.88 (1H, dd, H_e, $J = 8.4$, $J = 5.4$), 7.53 (2H, t, H₂ and H₁₀, $J = 6.6$), 3.74–3.64 (2H, m, CH₂), 2.53 (3H, s, CH₃CN), 1.44 (3H, t, CH₃, $J = 7.2$). MALDI-TOF MS: 687.0 [M – 2PF₆[−] – CH₃CN – H⁺]⁺. UV–vis (nm; H₂O): 276.0 (117 225 L mol^{−1} cm^{−1}), 362.1 (19 275), 373.8 (19 950), 452.8 (14 400).

[Ru(tpy)(dppz–CONHEt)(H₂O)](PF₆)₂ (9). An 8.8 mg (8.6 μmol) amount of **8** was dissolved in 0.6 mL of CD₃COCD₃–D₂O (2:1, v/v). The resulting solution was irradiated in a NMR tube with a Kodak slide projector (250 W halogen lamp) for 1 h and then transferred into a 25 mL round bottom flask for evaporation with the temperature not exceeding 30 °C. ¹H NMR (D₂O–CD₃COCD₃, 1:1, v/v): 10.13 (1H, d, H_a, $J = 5.2$), 10.01, 9.99 (1H, 2d, H_c, $J = 8.4$), 9.37, 9.35 (1H, 2d, H_d, $J = 8.0$), 8.99, 8.86 (1H, 2d, H_g, $J = 1.6$), 8.81 (2H, d, H₅ and H₇, $J = 8.2$), 8.71–8.46 (5H, m, H₄, H₈, H_b, 2H_h), 8.41 (1H, t, H_b, $J = 8.2$), 8.06 (2H, t, H₃ and H₉, $J = 8.0$), 7.99 (1H, d, H_f, $J = 5.5$), 7.93 (2H, d, H₁ and H₁₁, $J = 5.2$), 7.62 (1H, dd, H_e, $J = 7.9$, $J = 5.7$), 7.35 (2H, t, H₂ and H₁₀, $J = 6.7$), 3.63–3.50 (2H, m, CH₂), 1.34 (3H, t, CH₃, $J = 7.4$). MALDI-TOF MS: 687.0 [M – 2PF₆[−] – H₂O – H⁺]⁺. UV–vis (nm; H₂O): 274.3 (120 225 L mol^{−1} cm^{−1}), 361.0 (18 975), 375.2 (20 250), 477.0 (14 100).

Activated Ruthenium Complex 10. Compound **10** was obtained in a fashion similar to that for **7** starting from complex **5** (340 mg, 0.47 mmol) and was directly used for the coupling with compound **1**. R_f : 0.41 (D). Yield: 254 mg, 68%.

[Ru(tpy)(11)Cl](PF₆) (13). Ru(tpy)Cl₃ (189 mg, 0.43 mmol) and compound **11** (228 mg, 0.43 mmol) were heated at reflux for 4 h in 38 mL of EtOH–H₂O (3:1, v/v) containing LiCl (100 mg, 2.36 mmol) and Et₃N (95 μL) as a reductant. The mixture was evaporated to dryness

with a rotary evaporator and redissolved in 12 mL of EtOH–H₂O (5:1, v/v). The hexafluorophosphate salt of product was precipitated by the addition of aqueous saturated NH₄PF₆. An excess of ethanol was evaporated, and the mixture was kept at 4 °C overnight. The solid was filtered onto a fine-porosity frit, washed with cold water and diethyl ether, and air-dried (408 mg, 91%). *R*_f: 0.48 (B). ¹H NMR (CD₃CN): 10.62 (1H, d, H_a, *J* = 5.4), 9.84 (1H, m, H_c), 9.24 (1H, t, H_d, *J* = 8.2), 8.80 (1H, d, H_b, *J* = 9.6), 8.62 (2H, d, H₅ and H₇, *J* = 8.2), 8.55–8.41 (4H, m, H₄, H₈, H_b, H_h), 8.38 (1H, s, H_g), 8.23 (1H, t, H₆, *J* = 8.2), 7.93 (2H, t, H₃ and H₉, *J* = 7.9), 7.84 (1H, d, H_f, *J* = 5.2), 7.78 (2H, t, H₁ and H₁₁, *J* = 4.7), 7.50–7.42 (1H, m, H_c), 7.24 (2H, t, H₂ and H₁₀, *J* = 6.2), 3.78–3.40 (17H, overlapping m). MALDI-TOF MS: 901.2 [M – PF₆[–] – H⁺]⁺, 865.3 [M – PF₆[–] – Cl[–] – H⁺]⁺. UV–vis (nm; CH₃CN): 237.6 (51 350 L mol^{–1} cm^{–1}), 276.5 (96 650 L mol^{–1} cm^{–1}), 315.8 (49 350 L mol^{–1} cm^{–1}), 357.8 (20 000 L mol^{–1} cm^{–1}), 364.2 (20 000 L mol^{–1} cm^{–1}), 374.9 (20 850 L mol^{–1} cm^{–1}), 507.0 (15 000 L mol^{–1} cm^{–1}).

[Ru(tpy)(12)Cl](PF₆) (14). (a) Path A. Ru(tpy)Cl₃ (88 mg, 0.4 mmol) and compound **12** (167 mg, 0.2 mmol) were heated at reflux for 4 h in 18 mL of EtOH–H₂O (3:1, v/v) containing LiCl (47 mg, 1.1 mmol) and Et₃N (110 μL) as a reductant. The pot contents were filtered hot, and aqueous saturated NH₄PF₆ was added to the solution. The mixture was evaporated to dryness with a rotary evaporator and partitioned between CH₂Cl₂ and aqueous NaHCO₃. The aqueous phase was extracted with CH₂Cl₂ (three times), and all combined organic phases were then dried over MgSO₄ and evaporated. The crude material was silica gel chromatographed (0–8% EtOH in CH₂Cl₂) to give a brown foam (256 mg, 95%).

(b) Path B. Pyridine coevaporated compound **13** (284 mg, 0.27 mmol) was dissolved in dry pyridine (7 mL), and 4,4'-dimethoxytrityl chloride (157 mg, 0.46 mmol) was added. The mixture was stirred for 1.5 h at room temperature and then concentrated. The concentrate was poured into aqueous NaHCO₃, extracted with CH₂Cl₂, and dried over MgSO₄. The residue obtained after evaporation of the organic phase was silica gel chromatographed (0–8% EtOH in CH₂Cl₂). Yield: 203 mg, 56%.

(c) Path C. Solution of compound **1** (216 mg, 0.41 mmol) in dry DMF (3.8 mL) was added to the activated complex **10** (254 mg, 0.32 mmol) under nitrogen. The mixture was stirred for 2 h at room temperature and then concentrated. The residue was redissolved in 2 mL of EtOH, and the hexafluorophosphate salt of the product was precipitated by the addition of an ethanolic solution of NH₄PF₆ (5 mL). The resulting mixture was partitioned between CH₂Cl₂ and aqueous NaHCO₃. After extraction of the aqueous phase with CH₂Cl₂ all combined organic phases were then dried over MgSO₄ and evaporated. Silica gel chromatography (0–8% EtOH in CH₂Cl₂). Yield: 332 mg, 77%.

*R*_f: 0.59 (A), 0.86 (B). ¹H NMR (CDCl₃): 10.70 (1H, t, H_a, *J* = 5.4), 9.85, 9.76 (1H, 2d, H_c, *J* = 8.2), 9.20, 9.09 (1H, 2d, H_d, *J* = 8.2), 8.97, 8.87 (1H, 2s, H_b), 8.56–8.25 (7H, m, H₅, H₇, H₄, H₈, H_b, H_h, H_g), 8.06 (1H, t, H₆, *J* = 8.2), 7.85 (1H, d, H_f, *J* = 5.5), 7.73 (2H, t, H₃ and H₉, *J* = 7.6), 7.61 (2H, d, H₁ and H₁₁, *J* = 6.2), 7.34–7.04 (12H, m, H_e, H₂, H₁₀, DMT), 6.63–6.52 (4H, m, DMT), 4.20–4.05 (1H, m, DMTOCH₂CH), 3.82–3.61 (20H, overlapping m), 3.26–3.14 (2H, m, DMTOCH₂).

[Ru(tpy)(12–succinate)Cl](PF₆) (15) and Its Attachment to CPG. Compound **14** (205 mg, 0.15 mmol) and 4-(dimethylamino)pyridine (78 mg, 0.64 mmol) were dissolved in dry CH₂Cl₂ (2.5 mL). Then, succinic anhydride (62 mg, 0.62 mmol) was added, and the solution was stirred at room temperature for 6 h. The reaction mixture was first extracted with 0.1M citric acid followed by aqueous saturated NaHCO₃ solution. The organic phase was dried over MgSO₄ and evaporated. The crude product was purified by silica gel column chromatography eluting with 0–40% EtOH in CH₂Cl₂. Yield: 136 mg, 62%. *R*_f: 0.70 (B). ¹H NMR (CDCl₃–CD₃OD, 5:1, v/v): 10.61 (1H, t, H_a, *J* = 5.4), 9.92 (1H, d, H_c, *J* = 8.2), 9.36, 9.34 (1H, 2d, H_d, *J* = 8.2), 9.01, 8.90

(1H, 2s, H_b), 8.56–8.38 (7H, m, H₅, H₇, H₄, H₈, H_b, H_h, H_g), 8.21 (1H, t, H₆, *J* = 8.2), 7.87 (2H, t, H₃ and H₉, *J* = 7.8), 7.77 (1H, d, H_f, *J* = 5.4), 7.64 (2H, d, H₁ and H₁₁, *J* = 5.0), 7.41–7.14 (12H, m, H_e, H₂, H₁₀, DMT), 6.85–6.77 (4H, m, DMT), 5.24–5.14 (1H, m, DMTOCH₂–CH), 3.81–3.61 (20H, overlapping m), 3.23, 3.20 (2H, 2d, DMTOCH₂, *J* = 5.2), 2.66–2.56 (4H, m, CH₂CH₂ of succinyl).

To a solution of **15** (136 mg, 94 μmol) in dry acetonitrile (7.7 mL) was added 429 mg of aminopropyl CPG, *N,N*-diisopropylethylamine (1.64 mL, 9.4 mmol), benzotriazol-1-yloxytris(dimethylamino) phosphonium hexafluorophosphate (125 mg, 282 μmol), and *N*-hydroxybenzotriazole (38 mg, 282 μmol). The mixture was gently agitated at room temperature for 2 h; the CPG was filtered, washed (CH₂Cl₂), and assayed for loading of **13** (25 μmol/g resin). The excess of amino groups on the support was then acetylated with 3.3 mL of acetic anhydride–pyridine (9:1, v/v) containing 4-(dimethylamino)pyridine (64 mg) for 2 h. The support was then filtered and thoroughly washed with pyridine, CH₂Cl₂ (4 times), and diethyl ether (4 times) and then vacuum-dried. MALDI-TOF MS: 1 mL of concentrated aqueous NH₃ was added to 20 mg of the modified CPG and the mixture was shaken for 2 h at room temperature. The CPG was then removed by filtration and the filtrate was evaporated and analyzed giving *m/z* at 901.1, which corresponds to the mass of the compound **13** liberated from CPG and ionized as [M – PF₆[–] – H⁺]⁺.

[Ru(tpy)(11)(py)](PF₆)₂ (16). Into a 50 mL round bottom flask were placed 86 mg (92 μmol) of **13** (Cl[–] salt), 0.26 mL of pyridine, 9 mL of water, and 9 mL of ethanol. The mixture was refluxed with stirring for 5 h. The volume was then reduced by half with rotary evaporation, and a few milliliters of saturated aqueous NH₄PF₆ solution was added. The precipitate was collected by filtration, washed thoroughly with water and ether, and air-dried. Yield: 79 mg, 70%. ¹H NMR (acetone-*d*₆): 10.03, 10.00 (1H, 2d, H_a, *J* = 5.7), 9.54–9.49 (2H, m, H_c, H_d), 8.96–8.89 (3H, m, H_b, H₅, H₇), 8.79 (2H, d, H₄ and H₈, *J* = 7.7), 8.58–8.44 (4H, m, H_b, H_g, H_b, H_e), 8.23–8.14 (7H, m, H₃, H₉, H₁, H₁₁, H_f, pyridine), 7.98 (1H, t, pyridine, *J* = 7.9), 7.81–7.75 (1H, m, H_c), 7.49–7.42 (4H, m, H₂, H₁₀, pyridine), 4.00–3.91 (1H, m), 3.78–3.38 (16H, overlapping m). UV–vis (nm; CH₃CN): 231.3 (41 950 L mol^{–1} cm^{–1}), 278.8 (80 100 L mol^{–1} cm^{–1}), 302.5 (54 850 L mol^{–1} cm^{–1}), 363.4 (18 400 L mol^{–1} cm^{–1}), 373.4 (19 250 L mol^{–1} cm^{–1}), 475.9 (13 250 L mol^{–1} cm^{–1}).

[Ru(tpy)(11)(CH₃CN)](PF₆)₂ (17). Compound **13** (105 mg, 0.1 mmol) was refluxed under nitrogen in a CH₃CN–H₂O mixture (30 mL, 4:1, v/v) for 4 h. The reaction mixture was then filtered and concentrated to the volume of ~8 mL. A saturated solution of NH₄PF₆ was added, and the acetonitrile was evaporated. The precipitate was filtered, washed with water, and air-dried. The product was purified neutral alumina column chromatography eluting with first with CH₃CN–toluene (1:2, v/v), followed by pure CH₃CN. The last fraction was collected, and the solvent was removed by evaporation. Yield: 84 mg, 70%. ¹H NMR (acetone-*d*₆): 10.49 (1H, d, H_a, *J* = 5.4), 10.10, 10.08 (1H, 2d, H_c, *J* = 8.4), 9.58 (1H, t, H_d, *J* = 8.1), 9.18 (1H, d, H_b, *J* = 8.2), 9.06 (2H, d, H₅ and H₇, *J* = 8.2), 8.97–8.87 (3H, m, H_b, H₄, H₈), 8.78–8.63 (2H, m, H_b, H₆), 8.58 (1H, s, H_g), 8.29–8.23 (3H, m, H_f, H₃, H₉), 8.19–8.15 (2H, m, H₁ and H₁₁), 7.89, 7.86 (1H, 2t, H_e, *J* = 5.5), 7.54 (2H, t, H₂ and H₁₀, *J* = 6.4), 3.84–3.58 (17H, overlapping m), 2.53 (3H, s, CH₃CN). UV–vis (nm; CH₃CN): 278.0 (82 450 L mol^{–1} cm^{–1}), 302.1 nm (60 500 L mol^{–1} cm^{–1}), 363.6 nm (17 450 L mol^{–1} cm^{–1}), 372.0 nm (17 800 L mol^{–1} cm^{–1}), 457.2 nm (14 850 L mol^{–1} cm^{–1}).

[Ru(tpy)(11)(H₂O)](PF₆)₂ (18). (a) Path A. Compound **13** (202 mg, 0.19 mmol) and silver toluene-*p*-sulfonate (108 mg, 0.39 mmol) in acetone–water (8 mL, 3:1, v/v) were heated at reflux for 1 h. Silver chloride was filtered off, the solution volume was reduced to ~2 mL, and a few milliliters of saturated aqueous NH₄PF₆ solution was added. The precipitate was filtered, washed with little ice-cold water, and dried in vacuo. Yield: 171 mg, 75%.

(b) Path B. A 9.3 mg (7.8 μmol) amount of **17** was dissolved in 0.6 mL of D₂O–CD₃COCD₃ (2:1, v/v). The resulting solution was

irradiated in a NMR tube positioned in 3 cm in front of the lens of a Kodak slide projector (250 W halogen lamp) for 1 h and then transferred into a 25 mL round bottom flask to evaporate with the temperature not exceeding 30 °C.

¹H NMR (D₂O–CD₃COCD₃, 2:1, v/v): 10.09 (1H, d, H_a, *J* = 5.5), 9.86 (1H, d, H_c, *J* = 8.4), 9.15, 9.13 (1H, 2d, H_d, *J* = 6.9), 8.78–8.73 (3H, m, H₅, H₇, H_g), 8.65–8.52 (4H, m, H_b, H₄, H₈, H_h), 8.45–8.34 (2H, m, H_h, H₆), 8.03 (2H, t, H₃ and H₉, *J* = 7.9), 7.92–7.89 (3H, m, H₁, H₁₁, H_f), 7.46 (1H, dd, H_e, *J* = 8.2, *J* = 5.5), 7.36–7.31 (2H, m, H₂ and H₁₀), 3.83–3.40 (17H, overlapping m). UV–vis (nm; H₂O): 274.7 (11 9250 L mol⁻¹ cm⁻¹), 360.0 (20 800 L mol⁻¹ cm⁻¹), 375.3 (20 600 L mol⁻¹ cm⁻¹), 477.2 (15 300 L mol⁻¹ cm⁻¹).

Synthesis, Deprotection, and Purification of ODNs N, T, and I–IV. ODNs N, T, and I–IV were synthesized on 1.0 μmol scale with an eight-channel Applied Biosystems 392 DNA/RNA synthesizer using conventional 2-cyanoethyl phosphoramidite chemistry. Amino-modified ODNs II and IV were synthesized on amino-linker modified support. Phosphoramidite block 3 was dissolved in dry acetonitrile with a final concentration of 0.15 M and used after filtration for solid-phase synthesis of ODNs I, III, and IV with a coupling time of 10 min (25 s for standard nucleoside amidites). After each synthesis of the protected ODNs, the solid support was transferred directly out from the cassette to a 50 mL round bottom flask containing 20 mL of concentrated aqueous NH₃ and was shaken for 2 h at 20 °C. The CPG was then removed by filtration, and the filtrate was evaporated, redissolved in concentrated aqueous NH₃, and stirred at 55 °C for 17 h. The crude ODNs were purified by semipreparative RP-HPLC carried out on Kromasil 100 C18 column (5 μm) using a Bischoff equipment with pump Model 2250 and Spectrophotometer Lambda 1010 connected to CSW1.7 Chromatographic Station for gradient control. Gradient systems: A (0.1 M (Et₃NH)OAc, 5% MeCN, pH 7.0) and B (0.1 M (Et₃NH)OAc, 50% MeCN, pH 7.0). The ODNs purity was assayed by denaturing 20% polyacrylamide/7 M urea gel electrophoresis.

Coupling Procedure and Purification of Obtained ODNs V–VIII.

A 0.1 M concentration of Na₂B₄O₇ buffer (182 μL, pH 8.5) was added to the activated complex 7 (8.7 mg, 10 mmol) in a 1.5 mL Eppendorf tube. To this mixture was added 415 μL of H₂O followed by 597 μL of CH₃CN. After the addition of the amino-modified ODN (0.4 μmol) solution in H₂O (627 μL), the coupling was performed for 24 h in the dark at room temperature with slow shaking. The reaction mixture was then directly loaded onto a cation exchange Sephadex SP C-25 column (200 × 10 mm) and eluted with 30% CH₃CN/H₂O to remove excess of unconverted Ru²⁺ complex. The eluted orange-peel colored fraction was evaporated with the temperature not exceeding 30 °C and purified by RP-HPLC, as described above. Two fractions (a and b) isolated for each coupling were analyzed by ESI-MS: **Va**, 3912.8; **Vb**, 3913.4; **V1a**, 3912.5; **V1b**, 3913.8; **VII**, 3913.3, corresponding to [M – 3H⁺]⁻ ions of the mono-Ru²⁺-modified ODNs (the calculated *m/z* is 3913). MALDI-TOF MS: **Va**, 3872.6; **Vb**, 3871.9; **V1a**, 3872.5; **V1b**, 3871.8; **VII**, 3872.1, corresponding to [M – CH₃CN – 3H⁺]⁻ ions of the mono-Ru²⁺-modified ODNs; and **VIII**, 4798.4, corresponding to [M – CH₃CN – 5H⁺]⁻ ions of the bis-Ru²⁺-modified ODN. Purity of the Ru²⁺-ODN conjugates was also assayed by denaturing 20% polyacrylamide/7 M urea gel electrophoresis. Because of photosensitivity of ODNs V–VIII, they were handled in subdued light and stored in vials covered with black paper.

Automated Synthesis of ODNs VI. ODN VI was also prepared with DNA/RNA synthesizer using [Ru(tpy)(dppz)Cl]⁺-modified support and fast deprotecting amidites. After synthesis the CPG was treated with concentrated aqueous NH₃ at room temperature for 17 h and filtered off. The remaining filtrate was concentrated in vacuo with the temperature not exceeding 25 °C to remove ammonia. Concentrated aqueous solution was lyophilized to dryness and redissolved in 10 mL of CH₃CN–H₂O (1:1, v/v). The solution was heated at 55 °C for 17 h, in the course of which the color of the solution changed from purple-red to orange. After evaporation and HPLC purification the purity of

ODN VI was confirmed as described above. Two fractions (**V1a** and **V1b**) isolated in the course of HPLC purification were identified by ESI-MS: **V1a**, 3913.7; **V1b**, 3913.2, corresponding to [M – 3H⁺]⁻ ions of the mono-Ru²⁺-modified ODNs (the calculated *m/z* is 3913).

All prepared ODNs were subsequently sodium exchanged through a column of Dowex-50 Na⁺ form.

(II) MS Analysis of Ru²⁺-ODN Conjugates and Ru²⁺ Complexes. MALDI-TOF MS spectra were obtained using a Bruker REFLEX III (Bruker Daltonics, Bremen, Germany) fitted with a delayed extraction and a nitrogen laser (337 nm). A mixture (2:1) of 2,4,6-trihydroxyacetophenone (500mM in MeOH) and diammonium hydrogen citrate (100 mM in H₂O) was prepared and 1 μL deposited to dry on a target spot. The sample solution (1–3 μL in H₂O) containing ca. 100–300 pmol was mixed with 5 μL of the matrix/citrate mixture and 1 μL was applied on to the prepared sample spot. Most spectra were measured in the linear negative mode except for the products of binding of the Ru²⁺ complexes with dGMP and its derivatives, which were obtained in the reflectron positive mode. ESI-MS spectra were recorded using ESQUIRE-LC (Bruker Daltonics, Bremen, Germany) ion trap mass spectrometer. Typical samples containing ca. 100–200 pmol in H₂O (20 μL) were briefly (10 min) treated with Dowex(H⁺) beads. A 100 nmol amount of diammonium hydrogen citrate in H₂O and 2-propanol was added to obtain a 20% 2-propanol solution. The samples were introduced into the ion source by direct infusion at a rate of 2–3 μL/min maintained by a syringe pump. Negative ion spectra were collected at unit resolution and deconvoluted using Bruker's DA2 software.

(III) Molar Extinction of ODNs. The molar extinction coefficients (ε) of unmodified ODNs were calculated by nearest-neighbor method.⁴² For ODNs I, II, and IV the molar extinction coefficients were accepted to be equal to the ε of ODN N. The value of ε for ODN III was calculated as a sum of corresponding values for 5'-CTTAC-3' and 5'-CAATC-3'. Concentrations of Ru²⁺-ODNs were determined by accounting for the contribution to the absorbance at 260 nm from the [Ru(tpy)(dppz-L)(CH₃CN)]²⁺ moiety itself (Figure S2(C)). This was done by taking the ratio of the absorption of [Ru(tpy)(dppz-L)(CH₃CN)]²⁺ at 260 nm to that at 450 nm (*A*₂₆₀^{*}/*A*₄₅₀^{*}). The molar extinction coefficient for the Ru²⁺-ODNs (ε_{Ru}) was then calculated from the extinction coefficient (ε) for the corresponding amino-modified ODN using the formula

$$\epsilon_{\text{Ru}} = \epsilon \frac{A_{260}/A_{450}}{(A_{260}/A_{450}) - (A_{260}^*/A_{450}^*)}$$

where *A*₂₆₀ and *A*₄₅₀ are optical densities of Ru²⁺-ODN at 260 and 450 nm (λ_{max}), respectively.

(IV) Nucleoside Analysis of ODNs V–VIII by Their Enzymatic Digestion. To a 15.4 μL of aqueous solution of ODN (2 nmol) were added 10 μL of 1 M MgCl₂, 10 μL of AP buffer (500 mM Tris·HCl, pH 9.0), 1.5 μL (0.003 U/μL) of snake venom phosphodiesterase, 1 μL (20 U/μL) of alkaline phosphatase, and 75 μL of H₂O. The reaction mixture was incubated at 37 °C for 24 h, passed through a 0.45 μm Nylon syringe filter (Acrodisc), and analyzed by HPLC (Nucleosil 100–5C18 column, 4.6 × 200 mm, 5 μm RP-silica) with detection at 260 nm. HPLC mobile phases: A (0.1 M (Et₃NH)OAc, pH 7.0) and B (0.1 M (Et₃NH)OAc, 50% MeCN, pH 7.0). Peaks were identified by comparison with an authentic mixture of dC, T, and dA nucleosides. Nucleoside ratios were determined by integration of peak areas at 260 nm and normalization using the following molar extinction coefficients: 7300 (dC), 8800 (T), 15 400 (dA).

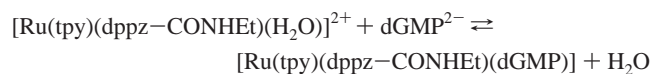
(V) UV–Vis Spectroscopic and Thermal Denaturation Studies. UV–vis: PC-computer interfaced Perkin-Elmer UV–vis spectrophotometer Lambda 40. Thermal denaturation experiments were performed

(42) (a) Cantor, C. R.; Warshaw, M. M.; Shapiro, H. *Biopolymers* **1970**, *9*, 1059–1077. (b) Fasman, G. *Handbook of Biochemistry and Molecular Biology*; CRC Press: Cleveland, OH, 1975; Vol. 1, p 589.

on the same UV–vis spectrophotometer with PTP-6 peltier temperature controller. UV melting profiles were obtained by scanning A_{260} absorbance versus time at a heating rate of 1.0 °C/min from 10 to 70 °C. The melting temperature, T_m (± 0.5 °C), was determined as the maximum of the first derivative of melting curves. The duplex melting experiments were performed in 1.3 mL of 20 mM Na₂HPO₄/NaH₂PO₄, 0.1 M NaCl, pH 7.0 buffer at hybrid concentration of ~ 1 μ M. After preparation, the solutions consisting of two components (for forming of duplexes) were heated to 85 °C for 5 min and then allowed to cool to 20 °C for 30 min under shaking. During the melting measurements at temperatures below ~ 15 °C, nitrogen gas was continuously passed through the sample compartment to prevent moisture condensation.

(VI) Photolysis Experiments on DNA–DNA Duplexes. The duplex photolysis experiments were performed in 20 μ L of 20 mM Na₂HPO₄/NaH₂PO₄, 0.1 M NaClO₄, pH 6.6 buffer at hybrid concentration of ~ 10 μ M. After mixing of two duplex forming components, containing 5'-³²P-labeled target strand **T** as a tracer, the solutions were heated to 85 °C for 5 min, allowed to cool to 20 °C for 30 min, and then irradiated with a Kodak slide projector (250 W halogen lamp) in a heavy-walled glass test tube (35 \times 6 mm o.d.) positioned in 3 cm in front of lens. After irradiation the reaction mixtures were lyophilized and analyzed by electrophoresis through a 20% polyacrylamide/7 M urea denaturing gel. DNA fragments were visualized and quantified by autoradiography using a Molecular Dynamics PhosphorImager.

(VII) Determination of the Equilibrium Constants for the Reaction between dGMP and [Ru(tpy)(dppz–CONHET)(H₂O)]-(PF₆)₂. The integrated form of the rate law equation for the reversible reaction



when the initial concentrations of the Ru²⁺ complex and dGMP are equal, can be expressed in the following form:

$$[\text{dGMP}] = [\text{dGMP}]_{\infty} + a/(\exp(bt) - c)$$

where parameters a – c are defined as

$$a = ([\text{dGMP}]_0 - [\text{dGMP}]_{\infty}) / (1 + k_1\tau([\text{dGMP}]_0 - [\text{dGMP}]_{\infty}))$$

$$b = \tau^{-1}$$

$$c = k_1([\text{dGMP}]_0 - [\text{dGMP}]_{\infty}) / (\tau^{-1} + k_1([\text{dGMP}]_0 - [\text{dGMP}]_{\infty}))$$

$[\text{dGMP}]_0$ and $[\text{dGMP}]_{\infty}$ correspond to the initial and equilibrium concentrations of dGMP,

k_1 is the rate constant for the forward reaction, and

τ is the relaxation time, after which the reaction system approaches the equilibrium in e time, i.e.

$$\text{when } [\text{dGMP}] = ([\text{dGMP}]_0 - [\text{dGMP}]_{\infty})/e + [\text{dGMP}]_{\infty}.$$

In accordance with that, the experimental concentration of dGMP, obtained in the course of a time dependence study, was approximated with a function $y = y_0 + a/(\exp(bx) - c)$ and $[\text{dGMP}]_{\infty}$ was accepted to be equal to calculated value for y_0 . Equilibrium constant was then calculated as

$$K = \frac{([\text{dGMP}]_0 - [\text{dGMP}]_{\infty})[\text{H}_2\text{O}]}{([\text{dGMP}]_{\infty})^2}.$$

Acknowledgment. We thank the Swedish Natural Science Research Council (Vetenskapsrådet), Swedish Engineering Research Council (TFR), and Philip Morris Inc. for generous funding.

Supporting Information Available: Reversed-phase HPLC purification of ruthenium conjugated ODNs and their precursors, UV–vis absorption spectra of various products resulting from various transformations, ESI and MALDI-TOF mass spectra of [Ru(tpy)(dppz)(CH₃CN)]²⁺–ODN conjugates, and PAGE pictures of various photocross linking products (PDF). This material is available free of charge via the Internet at <http://pubs.acs.org>.

JA0269486